

The cementitious performance of thermally activated recycled cement: a model system study



AUTHORS

Asghar Gholizadeh-Vayghan^{1*}, Guillermo Meza Hernandez², Felicite Kingne Kingne², Jun Gu², Nicole Dilissen^{2,4}, Snellings Ruben¹, Michael EL Kadi², Tine Tysmans³, Jef Vleugels⁴, Hubert Rahier²

¹ Sustainable Materials Management, Vlaamse Instelling voor Technologisch Onderzoek, 200 Boeretang, Mol, Belgium

² Physical Chemistry and Polymer Science, Department MACH, Vrije Universiteit Brussel, 1050 Brussels, Belgium

³ Department of Mechanics of Materials and Structures, Vrije Universiteit Brussel, 1050 Brussels, Belgium

⁴ Department of Materials Engineering, KU Leuven, Kasteelpark Arenberg 44, 3001, Heverlee, Belgium

* Correspondence: asghar.gholizadehvayghan@vito.be; Tel.: +32 14 33 57 57

ABSTRACT

This study was carried out as part of the Beton naar Hoogwaardig Beton Interreg Nederland-Vlaanderen project. In this research, the physico-chemical properties and cementitious performance of thermally activated cement pastes (referred to as DCP's) were investigated as a proxy of recycled concrete fines.

Hydrated pastes prepared from CEMI and CEMIII were subjected to four different dehydration conditions: 350 °C for 2 h, 550 °C for 2 h, 550 °C for 24 h, and 750 °C for 2 h, and milled to cement fineness. Particle characteristics, mineral composition, thermogravimetric response, and chemical reactivity of the DCP's (DCI and DCIII) were explored in relation to the original composition and the treatment (dehydration) conditions. The influences of incorporating the above materials in CEMI and CEMIII mixtures as SCM's were also investigated between 1 and 90 days through a systematic hydration study using thermogravimetric analysis, in-situ and ex-situ XRD and Rietveld analysis, isothermal calorimetry, and strength development assessment. The results suggest that thermal dehydration causes partial activation of the hydrated cement paste. Direct correlations could be observed between the dehydration temperature and time (in the studied ranges) and the grindability and BET fineness of the DCP, degree of crystallisation, formation of C₂S phases, and its chemical reactivity (per R3 test). The mechanical strength results suggest, however, that dehydration at 350 °C for 2 h generally results in the best pozzolanic performance. A possible discussion is provided for this observation in the text.

TABLE OF CONTENTS

Autors	I
Distribution list.....	Error! Bookmark not defined.
Summary	Error! Bookmark not defined.
Table of contents	III
List of figures	Error! Bookmark not defined.
List of tables.....	Error! Bookmark not defined.
List of graphs	Error! Bookmark not defined.
List of acronyms.....	Error! Bookmark not defined.
List of symbols	Error! Bookmark not defined.
1 Definition.....	Error! Bookmark not defined.
2 Description.....	Error! Bookmark not defined.
2.1 Title.....	Error! Bookmark not defined.
2.1.1 Title.....	Error! Bookmark not defined.
3 Conclusion.....	Error! Bookmark not defined.
3.1 Title.....	Error! Bookmark not defined.
3.1.1 Title.....	Error! Bookmark not defined.
List of literature	Error! Bookmark not defined.
References	Error! Bookmark not defined.
Annex A	Error! Bookmark not defined.

1 INTRODUCTION

The global warming has become the most concerning environmental crisis for the human civilization due to the increasing rates of natural catastrophes costing lives and other collateral damages across the globe with a worrisome perspective ahead. In the past 50 years, the greenhouse gas emissions have almost doubled while the cement industry has experienced a four-fold increase in the same [i]. The production of Portland cement continues to account for the highest share of anthropogenic CO₂ emission among all construction materials with 5 – 8 % CO₂ emission across the planet [ii,iii]. Clinker production is a CO₂ intensive process where 825 – 890 kg of CO₂ is generated for production of each ton of clinker [iv]. Approximately 50 % of such emission is caused directly by the calcination of limestone or other calcareous sources used as the raw feed; around 40 % is caused by the consumption of fossil fuels, and the remaining 10 % lends itself to the quarrying and transportation activities [v,vi]. The reduction in the use of clinker in new cement is known to be one of the most effective ways of lowering the CO₂ footprint of the concrete industry. Fly ash has by far been the most conventional supplementary cementitious material (SCM) used as partial cement replacement. However, due to the inevitable transition of the energy sector from fossil fuels, lack of fly ash for such application is expected in the near future calling for the need to find proper replacements for this SCM. On the other hand, the need and the merits of recycling and reuse of other industrial and urban wastes have become more evident and drawn a lot of attention in the recent decades.

One such source of waste with potential cementitious performance is the recycled concrete fines (RCF) with the most interesting ingredient being the hardened cement paste (HCP) adhering to the fine/crushed aggregates particles. RCF as the main concrete recycling by-products is usually not recommended for use in new concrete and has thus received limited attention from the construction industry [vii]. Researchers, however, realise that reactivation and reuse of the HCP present in RCF might effectively lower the environmental impact of the cement and concrete industry by reducing the clinker use in new concrete, and also reducing the concrete demolition waste. The joint climate actions and agreements to reduce the CO₂ emission have also further urged all stakeholders to move fast in this direction, which is why the research for valorisation of this by-product has rapidly expanded in the past years. A few different venues have been identified for the utilisation of RCF as a cement ingredient. Use of RCF as a raw feed in clinker production is one such approach. Gastaldi et al. (2015) [viii] investigated the use of recycled concrete powder as a raw feed for clinker production, and concluded that due to its composition, the use of RCF in clinker production should be limited to 20 % to 40 %. Schoon et al. (2014) point out that there are crucial differences between implementing the above approach on the lab scale and in the actual industrial scale [ix]. Due to the variations in the chemical composition of RCF, the use of this material as a raw feed in clinker production poses several challenges and is not easy to implement in the industrial scale.

Since complete hydration of cement does not usually take place, some unhydrated cement grains are always present in RCF, which can later contribute to hydration reactions. Direct use of milled RCF as partial cement replacement is as such studied in the past. However, solely relying on such limited hydration reactions is argued to be a low-end approach for using RCF as a cementitious material [x,xi]. Thermal treatment is reported to partially reactivate the adhered cement paste contained in RCF giving some cementitious properties to this material. Florea [xii] investigated the effects of using thermally activated recycled concrete fines as partial cement replacement on the strength of mortar mixtures. It was concluded that the very fine fraction of recycled concrete treated at 800 °C can be replaced for Portland cement up to 20 % without any significant loss of strength. Up to 20 % increase in the mechanical strength was also reported when replacing 10 % of blended cement containing high slag content with thermally dehydrated recycled concrete. Shui et al. (2009) [xiii] studied the effects of thermal

dehydration of hydrated cement paste (between 300 °C and 900 °C for 2.5 h) on its cementitious characteristics. They found a direct correlation between the dehydration temperature and the water demand and rate of setting of mixtures incorporating dehydrated HCP. They reported improvement in the cementitious performance of dehydrated HCP up to a dehydration temperature of 800 °C followed by a decline in the same. Wu et al. (2021) [xiv] also investigated the effects of applying thermal treatment on the properties and cementitious performance of waste concrete, mortar, and paste powder. They observed similar behaviour for all three materials concluding improvement in the performance of thermally treatment waste in comparison with untreated waste when the dehydration temperature ranged from 600 °C – 1000 °C. Inferior performance (compared to untreated waste) was observed when the dehydration temperature was as high as 1200 °C.

The objective of this report is to investigate the effects of thermal dehydration on the physico-chemical properties and cementitious performance of recycled concrete fines. Hydrated cement paste is used as a surrogate to RCF to eliminate the effects of aggregates on the results. HCP prepared from CEMI and CEMIII pastes are subjected to various dehydration temperatures ranging from 350 °C to 750 °C (durations studied: 2 or 24 h) and investigated for their grindability, fineness, thermogravimetric response, phase composition, and chemical reactivity. The cementitious performance of the above materials are also studied through a systematic hydration study and attempts are made to find correlations between the treatment conditions, material properties and cementitious performance.

2 MATERIALS AND METHODS

2.1 2.1. Materials selection and preparation

CEMI and CEMIII (prepared by blending 300 kg of CEMI with 220 kg of ground granulated blast furnace slag – GGBFS) were used for producing the initial hydrated cement pastes (later to be dehydrated and studied). **Error! Reference source not found.** shows the chemical, physical, and mineralogical properties of the CEMI, GGBFS, and CEMIII used in this research. A fine quartz filler was also used as a reference inert material to be compared with the thermally activated dehydrated cement paste (DCP) fines. **Error! Reference source not found.** shows the particle size distributions and the characteristic particle sizes of the above materials. Particle size distribution was measured using a Horiba laser diffraction particle size analyser in isopropyl alcohol (IPA).

For the preparation of the dehydrated cement fines, cement pastes with a water-to-binder ratio of 0.5 were first prepared from both CEMI and CEMIII. All pastes were cured in saturated lime water for 28 days at 21 ± 2 °C. Next, the hydrated cement pastes (HCPs) were crushed below 20 mm and dried at 40 °C for 48 h. The dried HCPs were then dehydrated at 1) 350 °C for 2 h, 2) 550 °C for 2 h, 3) 550 °C for 24 h and 4) 750 °C for 2 h, respectively. **Error! Reference source not found.** shows an overview of the dehydrated cement pastes produced for this study along with their labels. The materials were then transferred to a desiccator and cooled down to the room temperature. A planetary ball mill with a tungsten pot was used for milling the materials. All dried HCP samples were finally milled at 350 rpm for 14 min, characterised for their physico-chemical properties, and used for preparing new blended cement mixtures for further studies.

2.2 2.2. Characterisation methods

2.2.1 Materials characterisation

The particle size distribution of the milled dehydrated cement pastes and the starting materials was measured using a Horiba laser diffraction particle size analyser in IPA. Ultrasonication was applied to separate the particles in another IPA solution prior to characterisation. The reported results are the average of three measurements. The fineness of the DCP powders was also measured via the Brunauer-Emmett-Teller (BET) nitrogen gas sorption method using a Quantachrome Autosorb iQ Series instrument.

DCP powders were investigated using the scanning electron microscopy in order to explore the effects of the thermal pretreatment on the morphology of the DCP particles after milling. Image data were acquired using a FEI FEG Nova NanoSEM 450 equipped with a Bruker XFlash 5030 detector and secondary electron images at different magnifications were acquired at an electron acceleration voltage of 20 kV.

The bound water, portlandite, and carbonates contents of the DCP powders were measured via thermogravimetry in order to observe the effects of dehydration conditions on such parameters. Samples were heated at a 10 °C/min rate from 30 °C up to 1000 °C under nitrogen atmosphere at 50 ml/min flow rate. The bound water was determined by measuring the mass change between 50 °C and 550 °C, and the portlandite and carbonates contents were estimated respectively as the mass loss in the 400 °C – 500 °C and 600 °C – 790 °C ranges using the tangential method.

The phase composition of the DCP powders was determined via X-ray diffraction. The XRD data were collected using an Empyrean diffractometer (Panalytical) equipped with a CoK α tube. The tube operating conditions were 40 kV and 45 mA. Diffraction scans were recorded from 5 to 110 °2 θ , with step size 0.013 °2 θ , and a measurement time per step of 50 s. Rietveld analysis was performed using HighScore Plus software (version 4.6a) and the external standard approach was used to determine the amorphous phase content (rutile; Kronos 2300

TiO₂ external standard calibrated against NIST SRM 676a α -Al₂O₃). The starting crystal structure data are taken from Snellings (2016) [xv], and the chemical compositions of the dehydrated materials (calculated using **Error! Reference source not found.** data) were used to estimate the mass attenuation coefficients needed for the absorption correction.

The chemical (pozzolanic) reactivity of the DCP powders was also determined using the R3 (Rapid, Relevant, Reliable) reactivity test according to ASTM C1897. Synthetic pastes were produced incorporating the slags and Ca(OH)₂, H₂O, with additions of CaCO₃, K₂SO₄ and KOH to simulate the reaction medium of a hydrating Portland cement [9]. The designated amounts of DCP, calcium hydroxide, and calcite as shown in **Error! Reference source not found.** were weighed on weighing papers, homogenised, and stored at 40 °C. The dry mixture of the main ingredients was then mixed with the potassium solution at 1600 ± 50 rpm for 2 min using a high shear blender. The time of start of mixing was recorded as the ‘time zero’. A 15.0 g freshly made paste specimen was prepared and the cumulative heat was measured and recorded following ASTM C1897 – Method A procedure.

2.2.2 Hydration studies

A full hydration study was carried out on the dehydrated cement paste powders in comparison with the selected inert filler as follows. Cement pastes incorporating DCP powders were tested for their phase evolution (via X-ray diffractometry), heat evolution (via calorimetry), and thermogravimetric response (TGA). The control mixture was produced with 100 % CEMI or CEMIII with a water-to-binder ratio of 0.4. The blended mixtures were produced by replacing 30 % (mass) of the cement with either DCP of the same type. A mixture incorporating 30 % cement replacement with quartz powder as the inert filler was also produced to account for the nucleation effects of the DCPs. **Error! Reference source not found.** shows the compositions and labels of the produced pastes. All pastes were produced by first dry-mixing the powders for 60 min using a Turbula machine. The dry mixture of the main ingredients was then mixed with the water at 1600 ± 50 rpm for 2 min using a high shear blender so that a homogeneous paste was achieved.

All prepared cement pastes (see the compositions in **Error! Reference source not found.**) were exposed to extensive XRD investigations as follows. The early-age behaviour of all CEMI paste series were explored using in-situ XRD in 15-min time intervals shortly after preparation up to 24 h. The fresh pastes were cast into the XRD sample holders and covered with a semi-spherical X-ray transmissible polymer dome to avoid surface evaporation. The closed sample holder placed inside the XRD measurement position for continuous data collection during early hydration. Diffraction scans were recorded from 5 to 55 °2 θ under the conditions same as above. This was done to monitor the early-age formation of hydrated phases and allow the comparison of the effects of incorporating different DCP’s in cement pastes. The longer term evolution of hydration phases was also studied via ex-situ XRD from 1 d to 90 d for both CEMI and CEMIII pastes (from 5 to 90 °2 θ). The prepared cement pastes were cast into 12-mL plastic moulds and stored at 21 ± 2 °C for 24 h. Next, the hardened pastes were demoulded and stored inside slightly larger plastic bottles under a thin film of water until the testing age. At each testing age, the hardened pastes were taken out, a slice was cut, and the surface of the freshly cut specimen was smoothed using a 400 grit sandpaper and then flushed with water. The extra water film was removed from the surface and the specimen was directly subjected to the test under the conditions same as above.

The thermogravimetric response of the hydrated cements pastes was measured in order to determine and compare the bound water and portlandite contents of the control and blended pastes over time. Representative hydration-stopped samples were heated at a 10 °C/min rate from 30 °C up to 1000 °C under nitrogen atmosphere at 50 ml/min flow rate. The bound water was determined by measuring the mass change between 50 °C and 550 °C, and the portlandite content was estimated respectively as the mass loss in the 400 °C – 500 °C range using the tangential method.

A sample of each paste mixture per **Error! Reference source not found.** was prepared to determine the heat of hydration using isothermal calorimetry. The heat evolution was then monitored at 20 °C using a TAM Air calorimeter up to 7 days according to the Method B of ASTM C1702.

2.2.3 Mechanical performance

In order to assess the cementitious performance of the produced DCP's, standard mortar mixtures conforming to EN 196-1 specifications were produced and tested at different ages for their flexural and compressive strength. A water-to-binder ratio of 0.5 and a sand-to-binder ratio of 3.0 were assumed for all mixtures. The binder in the control mixtures was composed solely of either CEMI or CEMIII. In the case of test (blended) mixtures, 30 % mass replacement with each DCP was made in order to observe the influence of such replacements on the water demand and strength development of the mortars. For each CEM type, DCP's originally produced from the same CEM type were used as partial replacement. The mixture compositions are the same as those of the cement pastes (see **Error! Reference source not found.**). For each composition, sufficient amount of high-range water reducing admixture (also referred to as superplasticizer: SP) was added to the mixing water in order to maintain the mortar flow in the 200 ± 10 mm range. This approach was taken to eliminate the effects of DCP's on the consistence and compactability of the mixtures and its subsequent effects on the mechanical properties of the hardened mortars. Mixtures with flowability outside the designated ranges were disposed and new mixtures with adjusted superplasticizer contents were produced. Once the flowability in the desired range was obtained, the mixture was cast into three $40 \times 40 \times 160$ mm³ prismatic moulds, covered with plastic sheets and stored at 20 ± 2 °C for 24 h. Each mixture was produced four times (one batch for each testing age: 1, 7, 28, and 90 days). The hardened specimens were removed and cured in a climate chamber at 20 ± 1 °C and RH > 95 % until the age of testing. Upon curing, the specimens were first tested for their flexural strength, and the broken halves were then exposed to compressive strength test (all in accordance with EN 196-1).

3 RESULTS AND DISCUSSION

3.1 3.1. Material characterisation results

Error! Reference source not found. shows the particle size analysis results of the dehydrated cement paste powders along with the summarised characteristic particle sizes. It could be observed that the milled materials are in all accounts of similar size to the respective starting cement or finer (compare the characteristic particles sizes shown in **Error! Reference source not found.** with respective values in **Error! Reference source not found.**). Therefore, the applied milling energy was sufficient for producing DCP powder with suitable particle size. Comparing the particle size of DCPs produced under different treatment conditions, it could be concluded that an increase in the dehydration temperature and time generally leads to a higher grindability (note the order of the PSD curves in **Error! Reference source not found.** with respect to the colour codes). In the case of both CEMI and CEMIII, the DCP produced at 350 °C has the largest average particle size and D90 (see the blue curves), and DC/550°C/24h and DC/750°C/2h show the smallest values (see the blue and orange curves). The observed tendency for higher grindability with increased dehydration temperature and time can be attributed to the increased degree of dehydration in the hydrated phases (primarily C–S–H) which gradually causes structural damage to the microstructure of the hydrates thus enhancing their grindability. This could in turn lead to a higher fineness and/or porosity as well. The BET surface area values of both DCI and DCIII powders are shown in **Error! Reference source not found.**. It is observed in the case of DCI that the BET surface monotonically increases with increase in the dehydration time and temperature. Similar behaviour was also observed in the case of DCIII with the exception of DCIII/750°C/2h. A considerable decline in the BET surface area of DCIII is observed when the dehydration temperature exceeds 550 °C. It could be argued that as the dehydration temperature increases, the C–S–H continue to dehydrate and become more porous. However, once the dehydration temperature exceeds a certain level, a major part of C–S–H converts to C₂S which entails a collapse in the porous structure. This will later be confirmed by the Rietveld analysis results of the DCPs. An important finding from the BET results is that DCP (and consequently RCF) has a very high specific surface area as a potential SCM. The BET surface areas observed in the DCPs range from 15 m²/g to 23 m²/g, which is over one order of magnitude greater than those of the starting materials (i.e., CEMI and GGBFS: 1.76 and 1.35 m²/g, respectively). This is fuelled mainly by the porous structure of C–S–H, which only grows larger by application of a thermal treatment. Such high porosity could be considered a drawback for DCP/RCF as it increases the water demand of the binder. A closer look at the microstructure and morphology of the DCPs produced under different thermal conditions is provided in **Error! Reference source not found.** and **Error! Reference source not found.**. Each row contains a pair of images at 5,000 x and 50,000 x magnifications for the same DCP. It is observed that the DCPs grains have irregular shapes with flaky to cauliflower structures. It appears that the DCP produced at lower temperatures have more flaky appearance while those dehydrated at higher temperatures are more cauliflower-like (compare the different rows for both **Error! Reference source not found.** and **Error! Reference source not found.**). A highly porous appearance is observed in the case of DCIII/550°C/2h (see **Error! Reference source not found.**d), but this was not generally the case for this material and most likely not a significant observation. The BET surface area of this material also does not substantiate any outstanding feature in its porosity.

Error! Reference source not found.a and b show the TGA responses of DCI and DCIII prepared under different dehydration conditions, respectively. Using the TGA curves, the amounts of bound water, portlandite content, and carbonates content of DCI and DCIII are plotted in **Error! Reference source not found.**a and b, respectively. The first remarkable difference is found in the physical and chemical bound water contents of DCP's prepared at 350°C compared to those prepared at higher temperatures (for both DCI and DCIII). It could

be observed that with an increase in the dehydration temperature and time, the amounts of physical and chemical bound water, and portlandite content decrease in all cases. Notice the 50 – 400 °C responses of DCP's prepared at 350 °C in comparison with others. The portlandite contents of such DCP's were also found to be larger than those prepared at higher temperatures. It is interesting to note that the dehydration at no temperature has led to a complete decomposition of portlandite in neither case. This is later supported by the Rietveld analysis findings. However, a shift to the left (i.e., lower temperatures) is observed for the dehydration temperature of portlandite (notice the x-axis position of the DTG curves associated with portlandite peaks in **Error! Reference source not found.**a and b) with increase in DCP dehydration temperature and time. This might suggest that while a full decomposition of portlandite has not happened under any dehydration preconditioning, the portlandite structure is increasingly damaged during the such dehydration and is thus more readily dissociable. Minor mass losses were also observed at temperatures exceeding 600 °C, which could be due to the occasional formation of carbonates as a result of carbonation during the handling steps. However, the values appear to be generally negligible.

The mineral structure and phase composition of the above materials were also studied via X-ray diffractometry and the summarized Rietveld analysis results are presented in **Error! Reference source not found.** It can be clearly observed in both figures that the thermal treatment causes major drops in the amorphous contents of DCP's. This is to the most part due to the dehydration of C–S–H and its conversion to belite phases. Notice how the β -C₂S contents increase, especially at 750 °C. The γ -C₂S content also increases, to a smaller extent, as the dehydration temperature increases. No such phase was detected for DCP produced at 350 °C. The variations in the C₃S content appears to be within the error range and the inherent variability in the amount of this phase in different paste samples. Some increase in the C₃A and C₄AF contents were observed at 750 °C dehydration temperature. Moreover, it was noticed that the AFm and AFt phases were decomposed to the most part during the dehydration process at temperatures as low as 350 °C. No trace of such phases were observed at higher temperatures.

The changes in the phase compositions of the DCPs appear to entail some variations in their chemical reactivity. Depending on the treatment conditions, DCI and DCIII showed 7-d R3 reactivities in the ranges of 100 – 230 J/g and 220 – 300 J/g, respectively. The R3 heat release and heat flow results of DCI and DCIII materials are shown in **Error! Reference source not found.**a and b. Notice the differences in the heat release values of DCPs produced under different conditions. Dehydration at 350 °C yields the least reactive DCP in both cases. DCI produced at such temperature shows 45 % lower reactivity compared to other DCP, and DCIII shows 25 % lower reactivity. DCPs produced at higher temperatures show more or less similar reactivities. While DCI produced at 550°C/2h shows a significantly higher heat flow in short-term (compared to those produced at 550°C/24h and 750°C/2h), it falls slightly below at later times. DCIII/750°C/2h, on the other hand, shows slightly lower short-term reactivity but catches up at later times. Due to the calcination of portlandite, part of the generated heat at early hours is caused by the rehydration of calcium oxide, which is not a pozzolanic reaction. This is mainly the case for the DC produced at 550 °C and 750 °C. As such, one way to take this into account is to subtract the extra heat generated by the DCP produced at >350 °C (compared to that of DCP produced at 350 °C) during the first 2.5 h from the results. This is done separately for each DCP type and the 1 d, 3 d, and 7 d cumulative heat results are tabulated in **Error! Reference source not found.** An attempt was made to find correlations between the phase composition of the DCPs and their R3 heat release so as to determine which phases contribute the pozzolanic reactions or generation of heat. The analyses indicate that while all clinker phases have a positive influence correlation with the R3 heat release, no statistically significant correlation could be detected between such phases and this R3 test results (at 1, 3, or 7 days). Notice that the heat release values recorded for DCIII are greater than those of DCI in all cases. This is in spite of DCIII having lower clinker, β -C₂S, and portlandite contents. This is due to the reactions incurred by the residual (i.e., unhydrated)

GGBFS in DCIII. The strength and calorimetry results need to be explored to find out whether the above will have similar effects on the actual strength development or heat release of the mixtures prepared by DCIII compared DCI.

3.2 3.2. Hydration results

Error! Reference source not found. and **Error! Reference source not found.** show the TG and DTG plots of CEMI and CEMIII pastes, respectively. Notice that the pastes incorporating DCP's have generated a higher bound water compared to the pastes prepared by the inert material (i.e., quartz powder) at all ages which is an indication of more hydration products. Similar TG/DTG responses have been recorded for the pastes incorporating DCI compared to I-CTRL at early ages while they appear to experience more mass loss at later ages. This appears to be mostly associated with the bound water. In order to quantify the exact amounts of the bound water and portlandite, further calculations need to be made taking into account the effects of the cement replacement, and the bound water and portlandite originally contained in the DCP's. That is, the mixtures incorporating DCP contain some initial bound water, which contributes to the bound water values later measured on the hydrated pastes (same logic holds for the portlandite contained in the DCP's). As such, the bound water and portlandite present in DCP's (see **Error! Reference source not found.**) need to be subtracted from the measured bound water and portlandite contents in the pastes. Also, the values need to be normalised to the CEMI content in each paste for better comparison. As such, the values for I-CTRL are reported as is, while those of blended pastes are divided by 0.7 to account for the 30 % cement replacement. Similarly, in the case of CEMIII blends the values are divided by 0.577 (for III-CTRL) and by 0.4 (for the blended CEMIII mixtures) to normalise the masses to the amount of CEMI in each paste. The bound water and portlandite contents of the blended pastes produced with and without DCI and DCIII are plotted in **Error! Reference source not found.** and **Error! Reference source not found.**, respectively, taking into account all of the adjustments laid out above. It also shall be noted that the mass losses are reported as percent mass loss with respect to the residual masses at 550 °C. **Error! Reference source not found.**a suggests that the mixture containing quartz powder (I-QP) produces similar amounts of bound water compared to I-CTRL. The mixtures containing DCP's, however, contain considerably higher bound water compared to I-CTRL and I-QP (after accounting for the bound water contained in such DCP's). The highest bound water is observed in the case of I-550/24 followed by I-750/2, I-550/2, and finally I-350/2. I-550/24 also shows the highest portlandite content among the DCP-blended CEMI mixtures (see **Error! Reference source not found.**b) and the lowest portlandite is found in I-350/2.

Error! Reference source not found.a shows the bound water variations of different CEMIII pastes over time. In comparison with CEMI pastes, it is clearly observed that the CEMIII pastes have a slower rate of hydration reactions (due to the slower rate of bound water generation). Notice that unlike the case of CEMI mixtures, III-QP produces more bound water compared to III-CTRL at all ages (when normalised to the CEMI content). The early-age (i.e., ≤ 7 d) bound water contents of the CEMIII mixtures containing DCP are larger than those of III-QP and III-CTRL. This could be attributed to the accelerating effect of DCP on the hydration of cement (later supported by the calorimetry results). While some irregularities in the 28-d bound water results are observed, the 90-d bound water results are also indicative of the larger extent of hydration reactions in the case of DCP-blended mixtures compared to III-QP and III-CTRL. Despite the increasing trend of the portlandite content in the CEMI mixtures, the portlandite content in the CEMIII mixtures appears to decrease over time (in all cases). This is interpreted to be due to the presence of slag which consumes the portlandite over time, and in line with R3 reactivity test results. The lowest portlandite values are observed in the case of III-350/2 (which also showed the lowest bound water values). The higher bound water content and lower portlandite content of III-350/2 compared to III-QP could be indicative of more hydration

and pozzolanic reactions. This is reflected in the compressive strength results of such two mixtures as explained later.

The CEMI pastes were closely investigated in terms of their early-age phase evolution via in-situ X-ray diffractometry. As an example, **Error! Reference source not found.a** and **b** show the evolution of phases in the I-350/2 paste in the 8–15° 2 θ and 33–41° 2 θ ranges, respectively. **Error! Reference source not found.a** shows the formation of ettringite and hemicarboaluminates in the early hours of hydration. Notice how the clinker phases (A and B; alite and belite) react away over time giving rise to the formation of portlandite and other hydration phases. The in situ XRDs indicate more rapid and more extensive formation of ettringite in the cements blended with DCP treated at higher temperatures. Also the formation of AFm-hemicarboaluminate occurs significantly more early in blends with the higher temperature DCPs, this is a striking difference with the CEMI-control paste in which hemicarboaluminate was not observed in the in-situ experiment and is formed between one and seven days of hydration in the ex-situ measurements. Hemi-carboaluminate formation can be interpreted as indicative for low sulfate availability. Therefore; the earlier and more extensive formation of calcium aluminate hydrates in the DCP-blended cements may thus cause undersulfation and affect the subsequent hydration of C₃S and growth of C-S-H.

The longer term hydration of the DCP-cements shows broad similarities with the hydration of a reference Portland cement. Ettringite, portlandite and AFm phases form early on, while the AFm phases (hemi-, and monocarboaluminate) form subsequently. In the CEMIII blended cements, hydrotalcite is formed additionally as a reaction product of the slag.

The calorimetry results (cumulative heat and specific heat flow) of the CEMI pastes are plotted in **Error! Reference source not found..** It is observed that all mixtures containing DCP have a significantly higher heat flow in the initial hydration period (< 1.5 h) and a shorter induction period compared to I-CTRL and I-QP. Incorporation of all DCP's also expedite the acceleration period and the initial hydration reactions (notice the shift of the heat flow peaks to the left). With increase in the dehydration temperature and time, the heat flow peak shifts more to the left while the heat released in the acceleration and deceleration periods decreases. On the other hand, a secondary peak appears to form at later hours (8 – 24 h) which is more evident in I-750/2. Specifically in the case of this paste (i.e., I-750/2) and I-550/24 to some extent, a significant deviation in the heat release pattern from that of the control mixture is evident. Since the acceleration period is generally associated with the hydration of C₃S, and given the fact that all blended mixtures contain the same amount of C₃S (from CEMI clinker), such difference in heat release behaviour could be indicative of some retardation effect. Note that this retardation effect follows the initially higher rate of heat flow in the early hours. Higher initial heat release (< 2 – 4 h) is followed by a larger retardation effect (4 – 20 h) such that among all mixtures incorporating DCP, I-750/2 releases lower total heat compared to the control between 8 and 20 h. Such retardation does not translate to lower total heat release in long-term. Note that I-550/24 and I-750/2 show the highest heat release in 7 days (**Error! Reference source not found.b**). On the other side of the spectrum, I-350/2 shows the least deviation from the heat evolution of I-CTRL and the lowest total heat release among all blended mixtures. A good correlation could be established between the long-term heat release of the pastes incorporating each DCP and the R3 cumulative heat release of the same DCP's. However, this does not translate to higher strength results. **Error! Reference source not found.a – d** represent the absolute and relative strength development results of the CEMI mortar. The absolute strength results are shown in **Error! Reference source not found.a**. It is observed that I-550/24 and I-750/2 developed the lowest strength values among other mixtures containing DCP. This is while such DCP's (i.e., DCI/550°C/24h and DCI/750°C/2h) showed the highest heat release results both in the calorimetry and R3 tests. They also showed lower strength values compared to I-QP. I-350/2 and I-550/2, on the other hand, showed higher strength results compared to I-QP at all ages. In order to better understand the strength development behaviour of the mortar mixtures, the relative strength ratios are calculated with respect to the 90-d strength of each paste (**Error! Reference source not**

found.b), the strength of the control mortar at the same age (**Error! Reference source not found.c**), and the 90-d strength of the control mortar (**Error! Reference source not found.d**). According to **Error! Reference source not found.d**, the rate of (relative) strength development grows with increase in the dehydration temperature and time of the respective DCP. I-550/24 and I-750/2 have the highest rate of strength development followed by I-550/2h and finally I-350/2. **Error! Reference source not found.c** suggests that the relative strength ratio of the blended pastes at each age with respect to the strength of the control mixture at the same age is always the lowest for I-750/2 and I-550/24 (which are also lower than those of I-QP) and always remain below 60 %. This indicates that the influence of incorporating such DCP's on the strength of CEMI mixtures is beyond their dilution effect and even indicative of some non-compatibility with CEMI in the sense of strength development. I-550/2 and I-350/2, on the other hand, develop a 28-d compressive strength of nearly 70 % that of the control (but very close to that of I-QP), and continue to close the gap at later ages). Therefore, they could be deemed as moderately reactive SCMs. Mixtures incorporating DCI/350°C/2h, in particular, reach 85 – 90 % of the 28-d compressive strength of the control mixture which could be considered a satisfactory result given the high replacement ratio (30 %).

The calorimetry results of the CEMIII pastes are also shown in **Error! Reference source not found.**. A large peak observed in the case of III-QP is indicative of sulfate depletion (due to dilution effect), which is because CEMIII was prepared merely by combining CEMI and GGBFS without addition of calcium sulfates. Regarding the main pastes, similar heat evolution patterns as those of DCI-blended pastes could be identified for the DCIII-blended pastes with a few remarks. While all DCIII-blended pastes show a very high rate of heat evolution in the dissolution period (< 2 h), the shift of the acceleration peak to the left (compared to the control) is more severe when comparing each paste with the respective paste in the DCI-blended series (**Error! Reference source not found.**). While III-350/2 and III-550/2 show an initial peak at early hours, III-550/2 also shows a secondary peak at ~10 h which was not the case for I-550/2. III-350/2 also shows a minor secondary peak at 15 – 17 h. No initial peak in the heat flow of III-550/24 and III-750/2 could be identified while similar to III-550/2, a secondary peak around ~ 10 h could be observed for these pastes. All pastes incorporating DCIII exhibit higher heat of hydration compared to the control at all times while falling short from that of III-QP between 8 and 15 h. At later times, pastes incorporating DCIII show higher heat compared to both III-CTRL and III-QP and those incorporating DCP produced at higher dehydration temperatures and times generate higher heats. This is in agreement with the R3 results shown in **Error! Reference source not found.**. A close look at the strength development plots of the CEMIII mortar series (**Error! Reference source not found.**) reveal that the presence of slag causes some notable changes in the strength development behaviour of such binders. The first major observation is that the gap between the strength performance of the DCP-blended pastes compared to the control is much smaller in such blends compared to the CEMI series. All mixtures have also performed better than the mixture incorporating the inert filler (quartz powder) at all ages. III-550/24 has been found to develop the highest strength values compared to all DCP-blended mixtures at all ages, and even better than the control mortar at early ages (< 3 d). Such mixtures were also found to develop a 56-d strength exceeding the 28-d strength of the control mixtures. While the ratio of strength development is slower in the CEMIII mixtures compared to CEMI mixtures (compared **Error! Reference source not found.b** to **Error! Reference source not found.b**), the CEMIII specimens reach higher strength values at later ages in comparison with their respective CEMI mixtures. Such systematic behaviour suggests that recycling of concrete produced from CEMIII is technically more favourable when it comes to the long-term mechanical performance.

A more detailed comparison of the performance of the mixtures incorporating different DCIII materials reveals that there is not a remarkable added value in increasing the dehydration temperature of DCIII beyond 350 °C. It could be observed that III-350/2 and III-550/24 develop very similar 28-d and 90-d compressive strength results. The advantage of the latter appears to be limited only to the very early-age strength development (i.e., 1 d). Moreover, it could be

seen that increase in the dehydration temperature of DCIII to 750 °C has some detrimental effects on the strength development of the mixtures incorporating such material. Similar trend was observed for the CEMI pastes, and it could be therefore concluded that a thermal dehydration at 350°C for 2 h is sufficient for generating a suitable DCP and exceeding temperatures, especially beyond 550 °C, could result in adverse effects.

4 CONCLUSIONS

Dehydrated cement (DC) powders (referred to as DCP's) prepared from thermal treatment and comminution of CEMI and (synthetic) CEMIII pastes were investigated in this research for their physico-chemical properties and cementitious performance as SCMs. A full hydration study was carried out to explore the effects of partial replacement of fresh cement (both CEMI and CEMIII) with such SCMs. The main findings of this research are summarised as follows:

- Increase in the dehydration temperature from 350 °C to 750 °C generally results in an increase in the grindability of such materials as well as their surface area (with an exception observed in the case of DCIII dehydrated at 750 °C).
- According to both TGA and Rietveld analysis results, a full decomposition of portlandite does not take place in the DCP's even at dehydration temperatures as high as 750 °C. This may be related to rehydration and carbonation of free lime by contact with ambient air during subsequent processing (milling) and storage. Free lime, while expected to form, was never found in the DCPs.
- Dehydration of C–S–H at 350 °C does not result in the formation of γ -C₂S while such phase was detected for the DCP's dehydrated at higher temperatures. Residual B-C₂S, on the other hand, was detected at all dehydration temperatures. The content of potentially hydraulic phases increased with dehydration temperature at the expense of an amorphous or nanocrystalline phase (likely C-S-H and other cement hydrates).
- According to the R3 results, DCP's prepared at higher dehydration temperatures and times tend to generate significantly higher initial rates of reaction compared to those prepared at lower temperatures. They were also found to generate larger heats in the long term (after 1 – 2 days) compared to the same.
- A direct correlation was found between the R3 heat results and the amount of potentially hydraulic phases formed in the DCP's (for both DCI and DCIII). The amorphous content of the DCP's were also found to significantly decrease with increase in the dehydration temperature and time.
- Pastes incorporating DCP generated higher bound water and portlandite content compared to the control paste (i.e., I-CTRL). The pastes incorporating DCP's prepared at higher temperatures generated higher bound water compared to the other blended pastes, but this did not translate to a better strength performance.
- Incorporation of DCP in the pastes results in a very high initial heat generation in the first 1 – 2 h and also expedites the acceleration period. However, the pastes incorporating DCPs produced at higher temperatures (i.e., 550°C/24h and 750°C/2h) have significantly lower heat generation in the main hydration period, and tend to generate more heat at later hours.
- The best strength performance in the case of CEMI pastes was observed for DCI/350°C/2h followed by DCI/550°C/2h, 550°C/24h, and 750°C/2h. As such, dehydration at temperatures exceeding 350 °C is not recommended for this DC type.
- In the case of CEMIII pastes, while DCIII/550°C/24h showed the best early-age strength performance, similar strength activity was identified for DCIII/350°C/2h at later ages (after 28 d). Increasing the dehydration temperature to 550 °C for extended durations of time is not justifiable unless high early-age strength is desired.

5 LIST OF TABLES

Table 1. The chemical compositions of the binder materials

Table 2. Overview of the studied dehydrated cement samples

Table 3. Overview of the blended cement compositions (values in mass %)

Table 4. The batched masses of R3 mixtures produced for studying the chemical (pozzolanic) reactivity of the dehydrated cement paste powders

Table 5. The corrected R3 cumulative heat results for the dehydrated cement paste powders

6 LIST OF FIGURES

Figure 1. The particle size distribution of the raw materials

Figure 2. The particle size distribution of the dehydrated cement paste powders treated under different conditions

Figure 3. BET surface areas of the dehydrated cement paste powders treated under different conditions.

Figure 4. SEM images of the DCI dehydrated cement paste powders at 5,000x (left) and 50,000x (right) magnifications. (a): 350°C/2h, (b): 550°C/2h, (c): 550°C/24h, (d): 750°C/2h

Figure 5. SEM images of the DCIII dehydrated cement paste powders at 5,000x (left) and 50,000x (right) magnifications. (a): 350°C/2h, (b): 550°C/2h, (c): 550°C/24h, (d): 750°C/2h

Figure 6. TGA and DTG plots of the dehydrated cement paste powders. (a): DCI, (b): DCIII

Figure 7. Bound water, portlandite, and calcium carbonate content of the dehydrated cement paste powders. (a): DCI, (b): DCIII

Figure 8. Rietveld analysis results of the dehydrated cement paste powders. (a): DCI, (b): DCIII

Figure 9. The R3 cumulative heat release and specific heat flow plots of dehydrated cement paste powders in the first 24 h (left) and 7 days (right). (a): DCI, (b): DCIII

Figure 10. The TGA and DTG curves of the CEMI pastes. (a) 3 d, (b) 7 d, (c) 28 d, (d) 90 d

Figure 11. The TGA and DTG curves of the CEMIII pastes. (a) 3 d, (b) 7 d, (c) 28 d, (d) 90 d

Figure 12. The bound water (a) and portlandite content (b) values of the CEMI pastes (values normalised to the CEMI content in the pastes)

Figure 13. The bound water (a) and portlandite content (b) values of the CEMIII pastes (values normalised to the CEMI content in the pastes)

Figure 14. The in-situ XRD pattern of I-350/2 paste over time. (a): 8–15°, (b): 33–41°; A: alite, B: belite, E: ettringite, F: ferrite, H: hemicarboaluminates, P: portlandite

Figure 15. The ex-situ XRD pattern of (a) I-350/2 paste, and (b): III-350/2 pastes over time; A: alite, AF: AFm phases, B: belite, C: C₃A; E: ettringite, F: ferrite, H: hemicarboaluminates, M: monocarboaluminates; P: portlandite, Q: quartz, T: hydrotalcite

Figure 16. The ex-situ XRD pattern of (a) I-350/2 paste, and (b): III-350/2 paste at 28 d; A: alite, AF: AFm phases, B: belite, C: C₃A; E: ettringite, F: ferrite, H: hemicarboaluminates, M: monocarboaluminates; P: portlandite, Q: quartz, T: hydrotalcite

Figure 17. The calorimetry results of CEMI pastes (a) up to 24 h and, (b): up to 7 d

Figure 18. The calorimetry results of CEMIII pastes (a) up to 24 h and, (b): up to 7 d

Figure 19. The compressive strength results of the CEMI pastes. (a) absolute compressive strength results with error bars ($\approx 2 \times$ standard deviation), (b) relative strength ratios with respect to the 90-d strength of each respective paste, (c) relative strength ratios with respect to the strength of the control mixtures at the same age, (d) relative strength ratios with respect to the 90-d strength of the control mixture

Figure 20. The compressive strength results of the CEMIII pastes. (a) absolute compressive strength results with error bars ($\approx 2 \times$ standard deviation), (b) relative strength ratios with respect to the 90-d strength of each respective paste, (c) relative strength ratios with respect to the strength of the control mixtures at the same age, (d) relative strength ratios with respect to the 90-d strength of the control mixture

Table 1. The chemical compositions, physical properties, and mineral compositions of the binder materials

Quantity	Content (m%)		
	CEM I	GGBFS	CEM III
CaO	60.7	37.5	51.8
SiO ₂	18.5	34.5	24.3
Al ₂ O ₃	4.89	14.4	8.11
MgO	1.63	7.84	4.19
Fe ₂ O ₃	2.88	0.40	1.85
TiO ₂	0.31	1.29	0.55
MnO	0.05	0.31	0.18
SO ₃	2.53	1.23	2.00
K ₂ O	0.84	0.74	0.74
Na ₂ O	0.12	0.47	0.22
Na ₂ O _{eq}	0.67	0.96	0.71
C ₃ S M3	59.5	–	33.8
β-C ₂ S	17.1	–	9.1
C ₃ A cubic	5.2	–	2.8
C ₄ AF	10.0	–	6.1
Portlandite	1.3	–	0.1
Gypsum	1.6	–	0.8
Anhydrite	0.9	–	0.2
Basanite	3.1	–	1.6
Quartz	0.6	–	0.17
Periclase	0.7	–	0.61
Amorphous	0.0	100	44.7
LOI (%)	1.47	0.97	1.95
SSA (m ² /g)*	1.76	1.35	1.42

* BET specific surface area

Table 2. Overview of the studied dehydrated cement paste samples

Starting material	Long name	Dehydration temperature (°C)	Dwelling time (h)
CEM I	DCI/350°C/2h	350	2
	DCI/550°C/2h	550	2
	DCI/550°C/24h	550	24
	DCI/750°C/2h	750	2
CEM III	DCIII/350°C/2h	350	2
	DCIII/550°C/2h	550	2
	DCIII/550°C/24h	550	24
	DCIII/750°C/2h	750	2

Table 3. Overview of the blended cement compositions (values in mass %)

Long name	CEM I	CEM III	Quartz powder	DC/350°C /2h	DC/550°C /2h	DC/550°C /24 h	DC/750°C /2h
I-CTRL	100	–	–	–	–	–	–
I-QP	70	–	30	–	–	–	–
I-350/2	70	–	–	30	–	–	–
I-550/2	70	–	–	–	30	–	–
I-550/24	70	–	–	–	–	30	–
I-750/2	70	–	–	–	–	–	30
III-CTRL	–	100	–	–	–	–	–
III-QP	–	70	30	–	–	–	–
III-350/2	–	70	–	30	–	–	–
III-550/2	–	70	–	–	30	–	–
III-550/24	–	70	–	–	–	30	–
III-750/2	–	70	–	–	–	–	30

Table 4. The batched masses of R3 mixtures produced for studying the chemical (pozzolanic) reactivity of the dehydrated cement paste powders

Slag (g)	Ca(OH) ₂ (g)	Potassium solution (g)	CaCO ₃ (g)
11.12	33.33	59.94	5.56

Table 6. The corrected R3 cumulative heat results for the dehydrated cement paste powders

DCP label	1 day	3 day	7 day
DCI/350°C/2h	95	115	125
DCI/550°C/2h	175	196	204
DCI/550°C/24h	137	177	189
DCI/750°C/2h	143	192	210
DCIII/350°C/2h	138	193	225
DCIII/550°C/2h	185	240	271
DCIII/550°C/24h	180	243	283
DCIII/750°C/2h	160	237	281

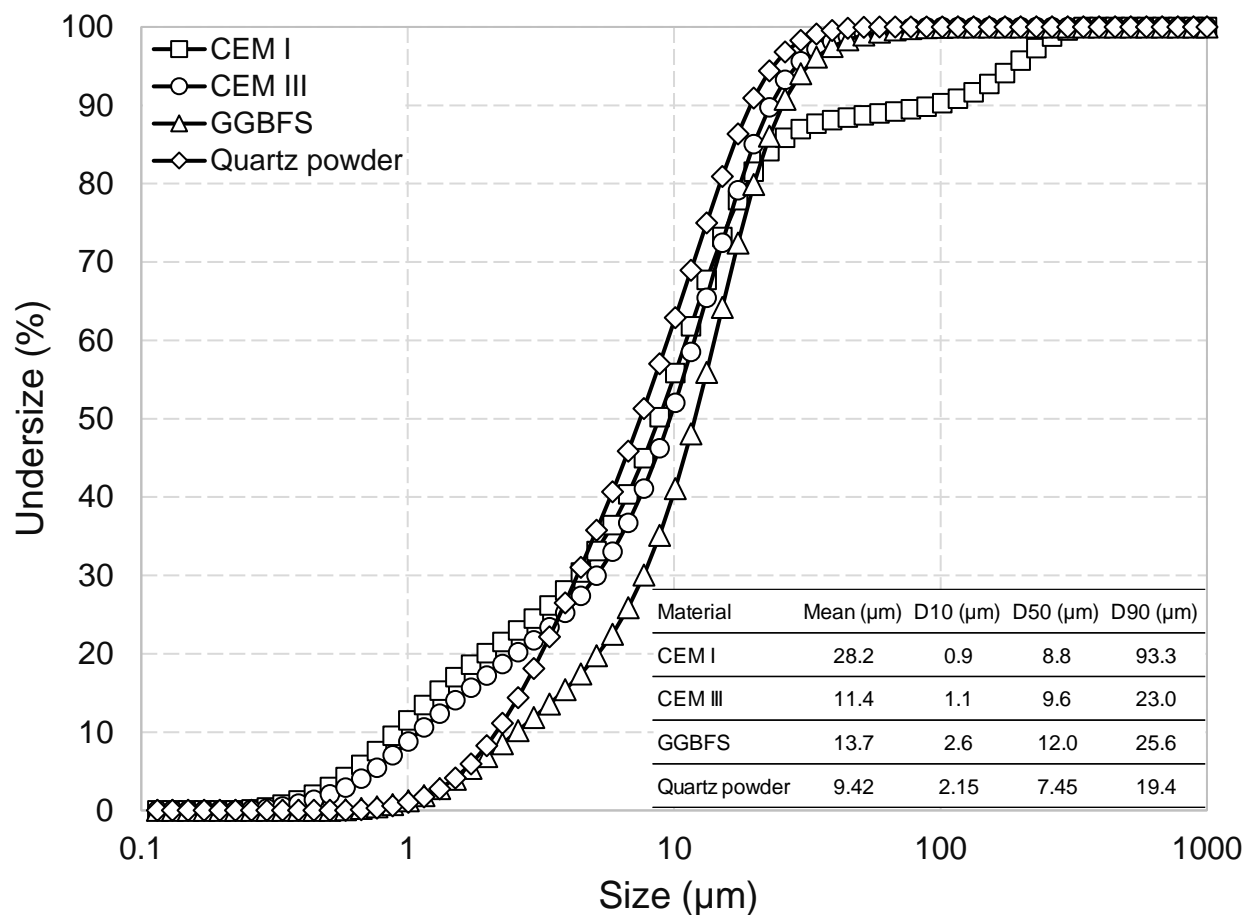


Figure 1. The particle size distribution of the raw materials

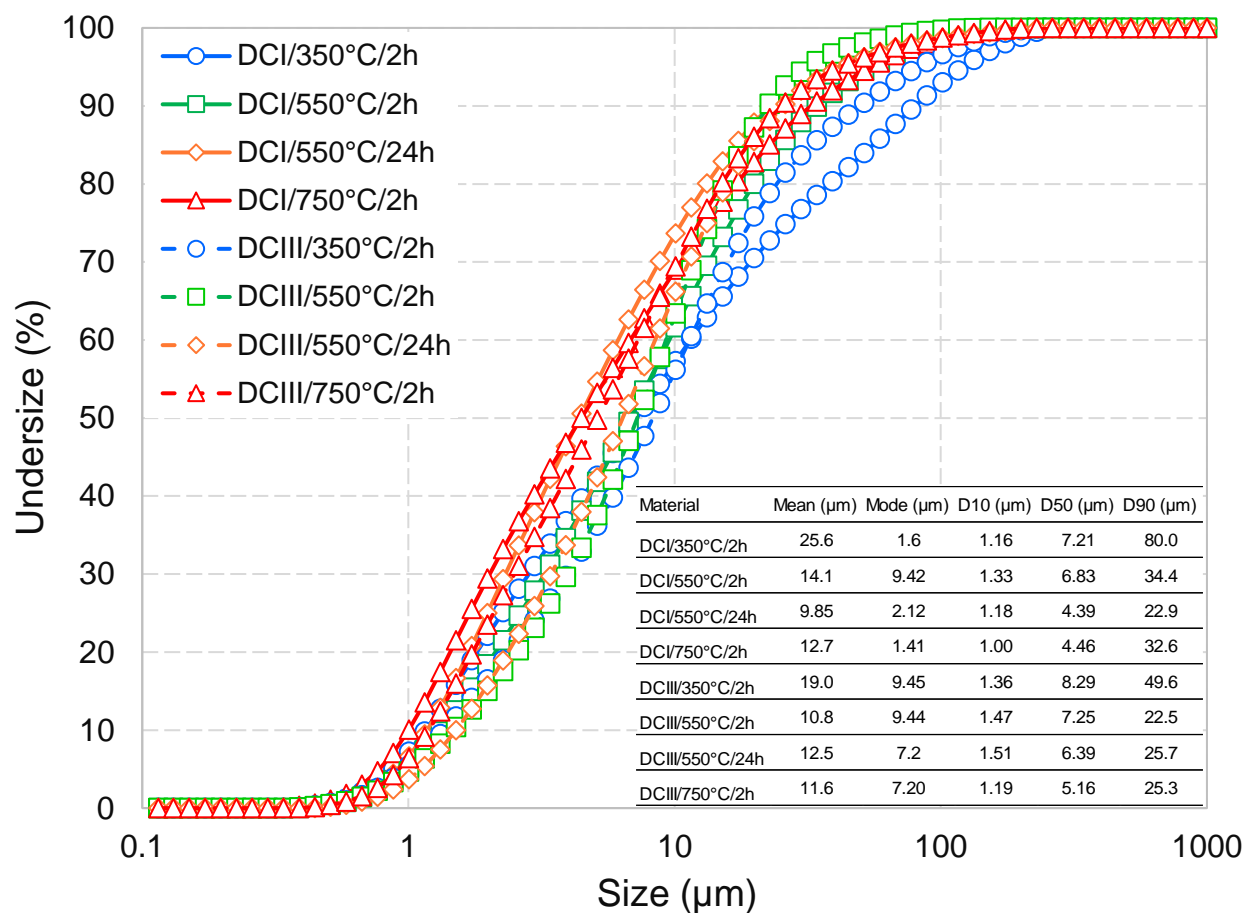


Figure 2. The particle size distribution of the dehydrated cement paste powders treated under different conditions

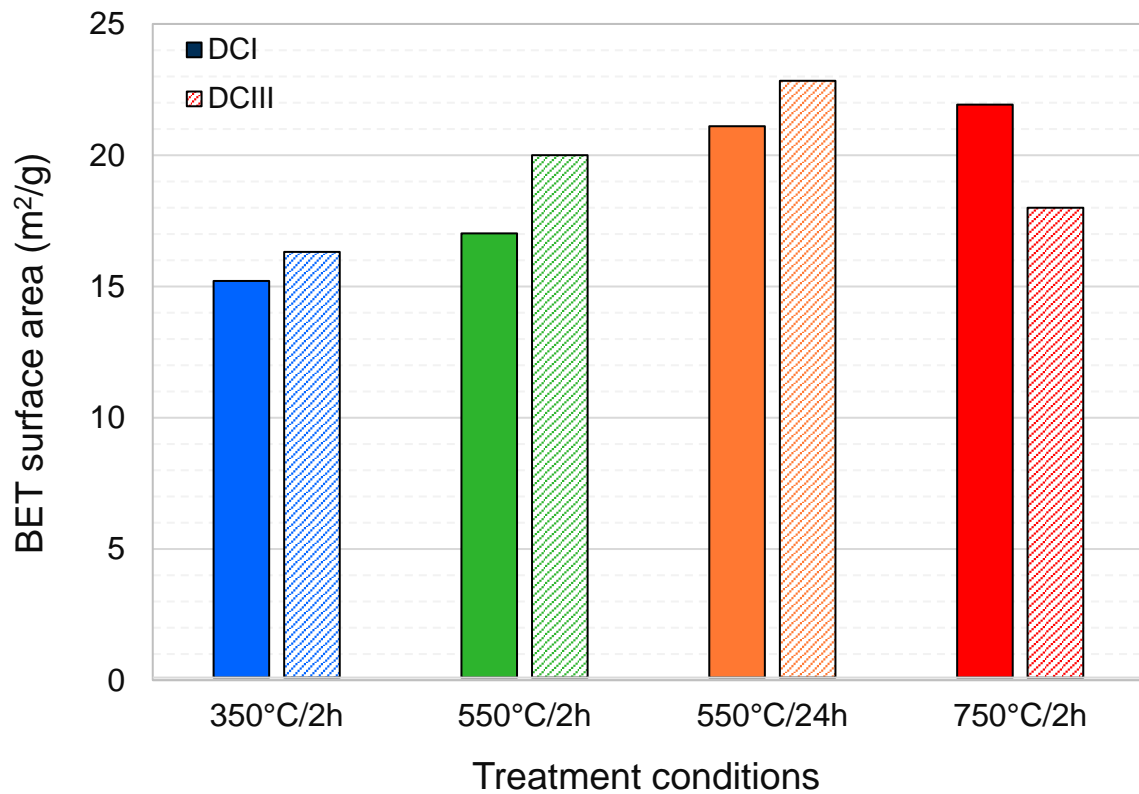


Figure 3. BET surface areas of the dehydrated cement paste powders treated under different conditions

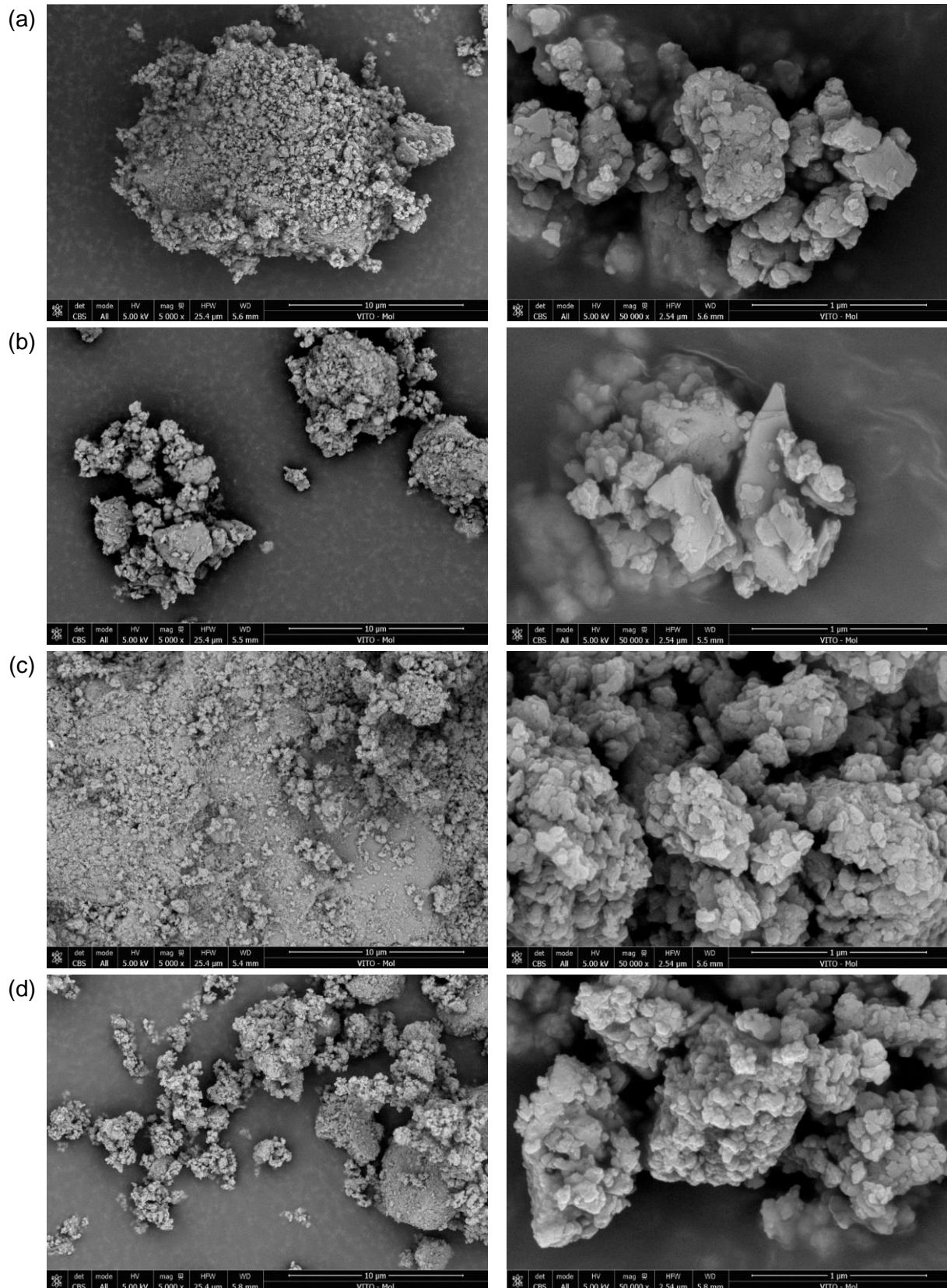


Figure 4. SEM images of the DCI dehydrated cement paste powders at 5,000x (left) and 50,000x (right) magnifications. (a): 350°C/2h, (b): 550°C/2h, (c): 550°C/24h, (d): 750°C/2h

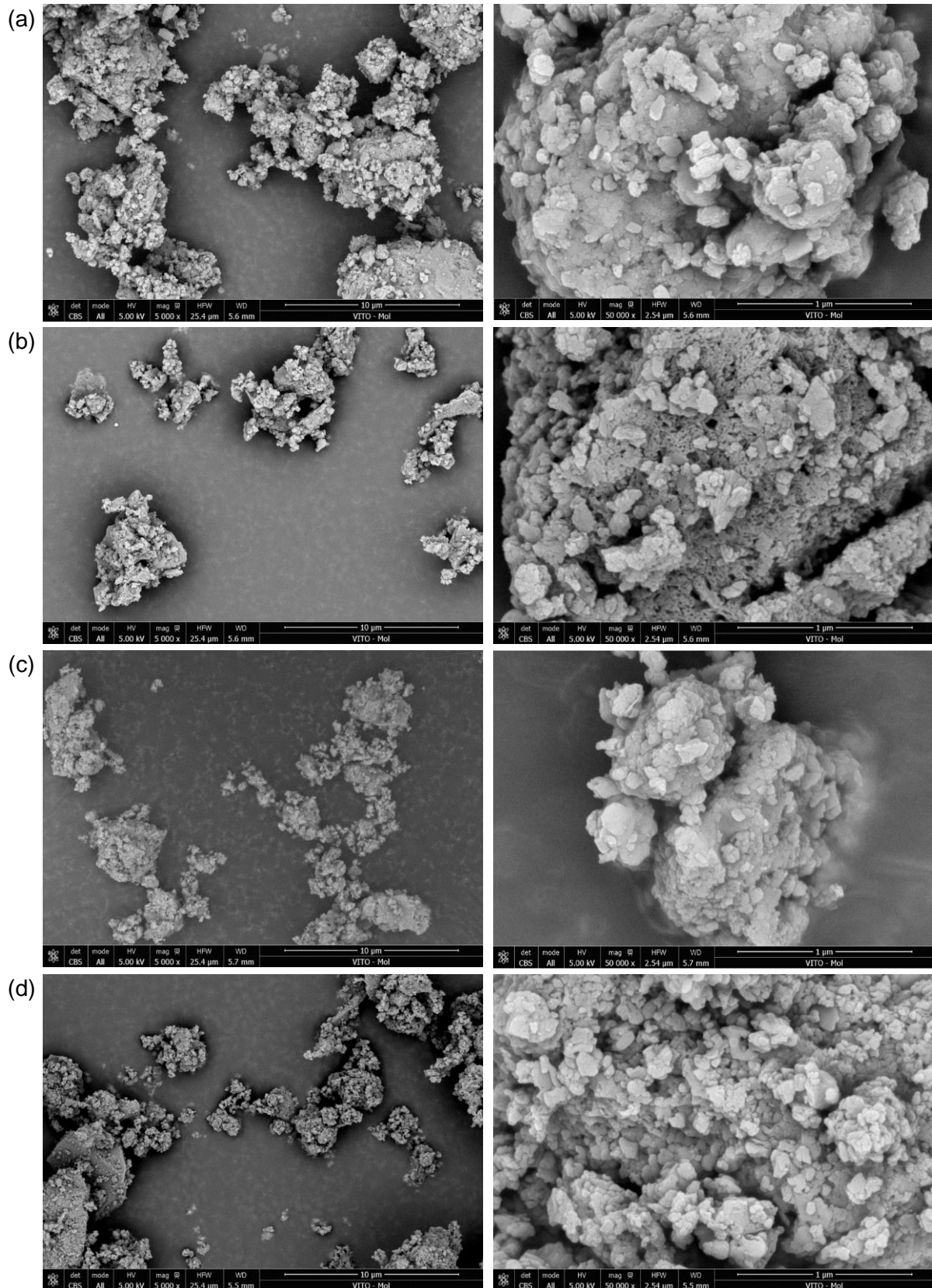


Figure 5. SEM images of the DCIII dehydrated cement paste powders at 5,000x (left) and 50,000x (right) magnifications. (a): 350°C/2h, (b): 550°C/2h, (c): 550°C/24h, (d): 750°C/2h

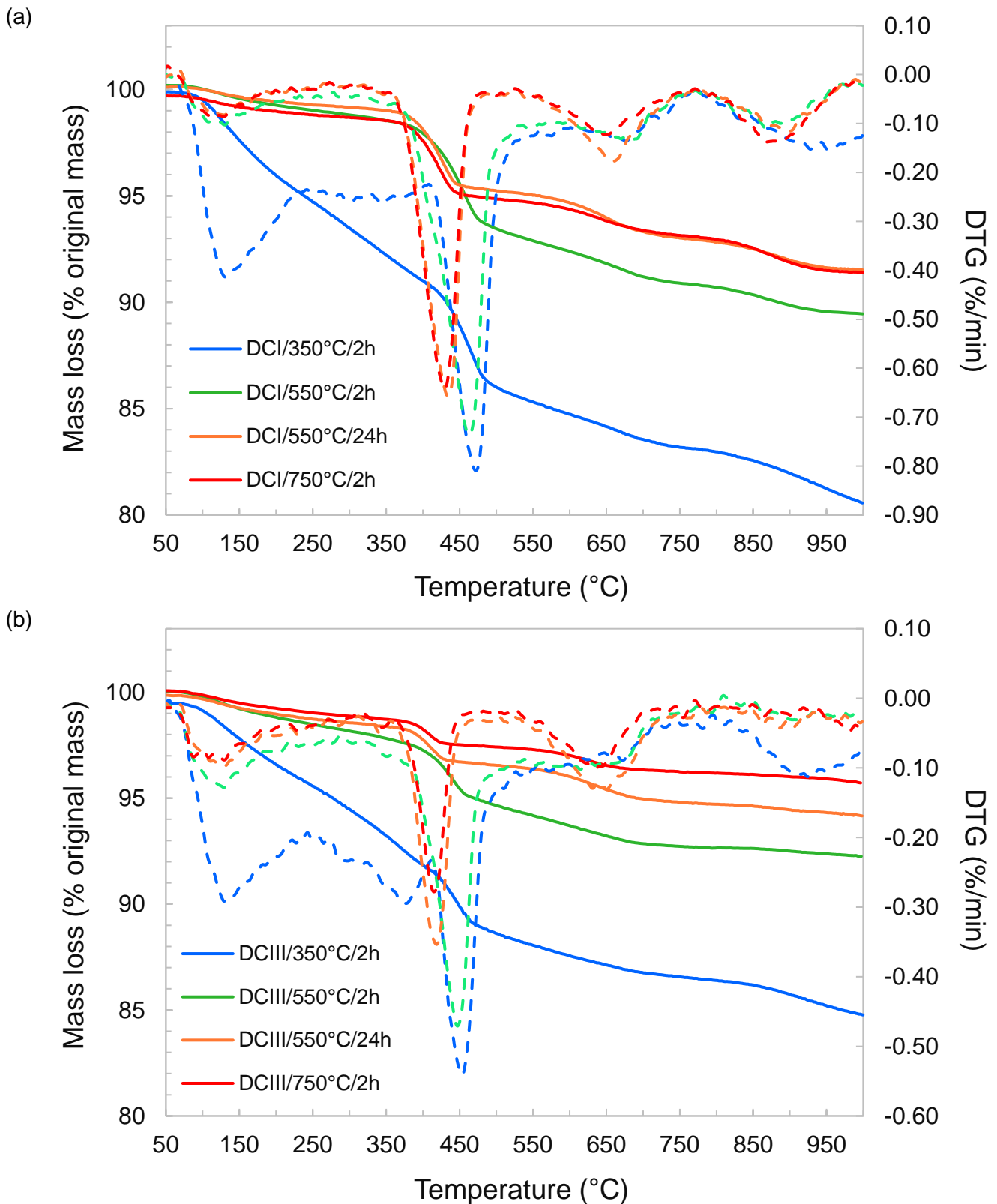


Figure 6. TGA and DTG plots of the dehydrated cement paste powders. (a): DCI, (b): DCIII

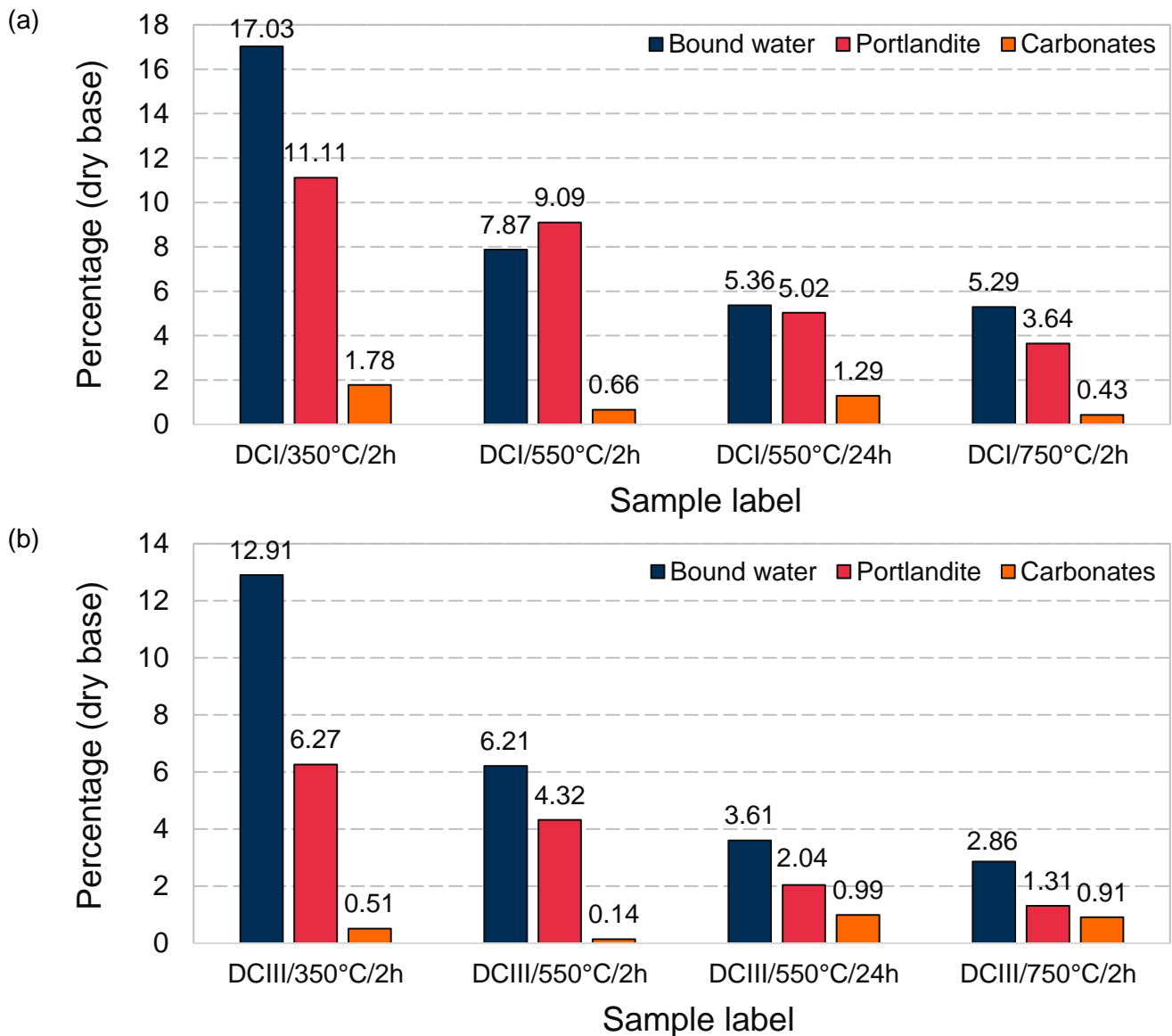


Figure 7. Bound water, portlandite, and carbonates contents of the dehydrated cement paste powders. (a): DCI, (b): DCIII

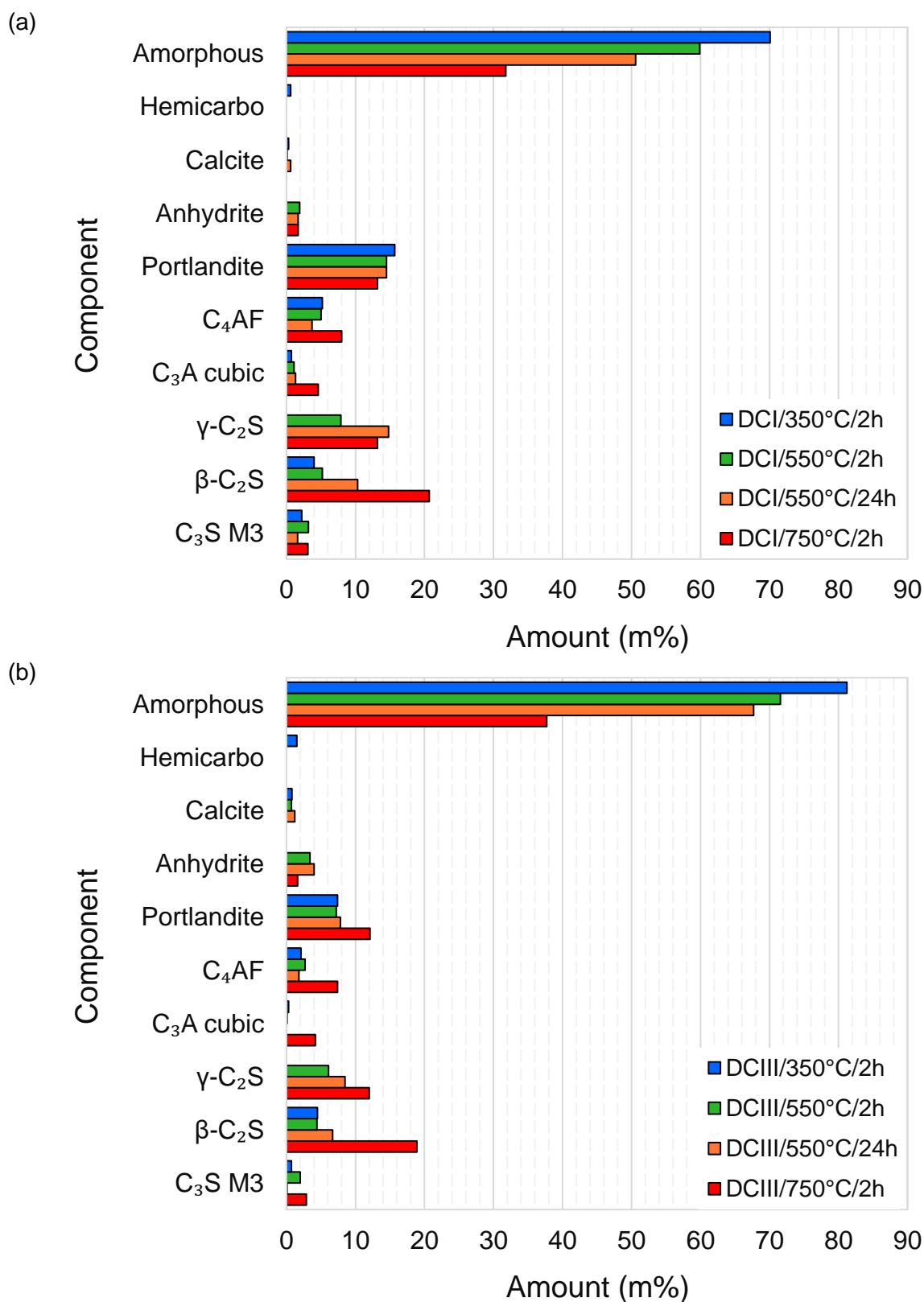


Figure 8. Rietveld analysis results of the dehydrated cement paste powders. (a): DCI, (b): DCIII

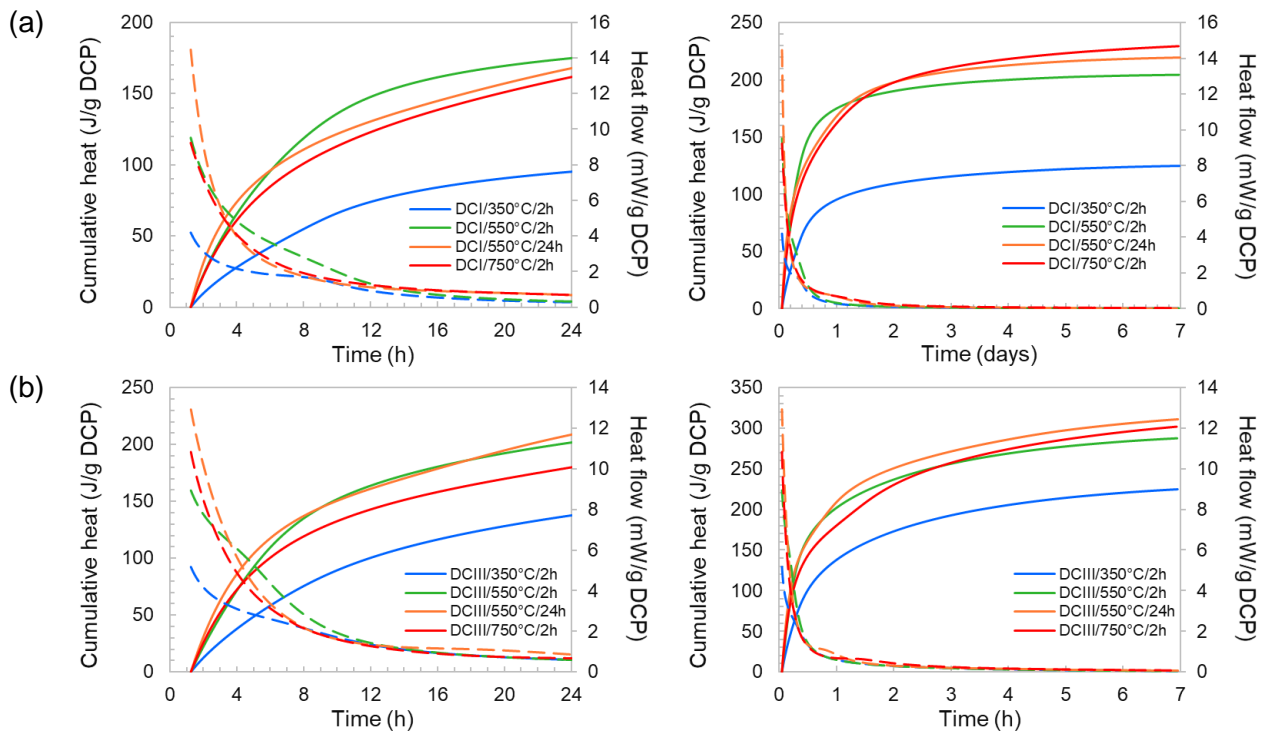


Figure 9. The R3 cumulative heat release and specific heat flow plots of dehydrated cement paste powders in the first 24 h (left) and 7 days (right). (a): DCI, (b): DCIII

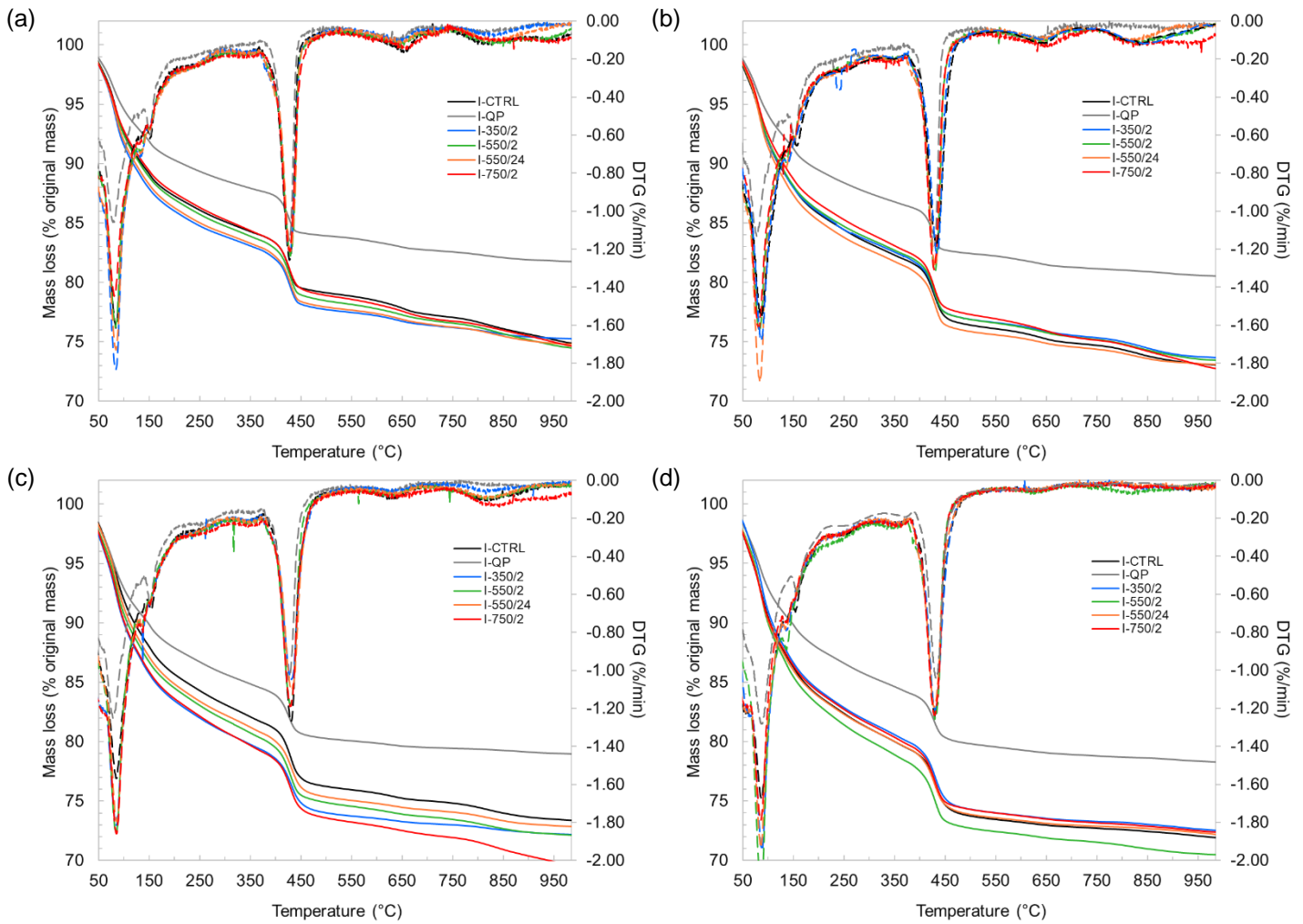


Figure 10. The TGA and DTG curves of the CEMI pastes. (a) 3 d, (b) 7 d, (c) 28 d, (d) 90 d

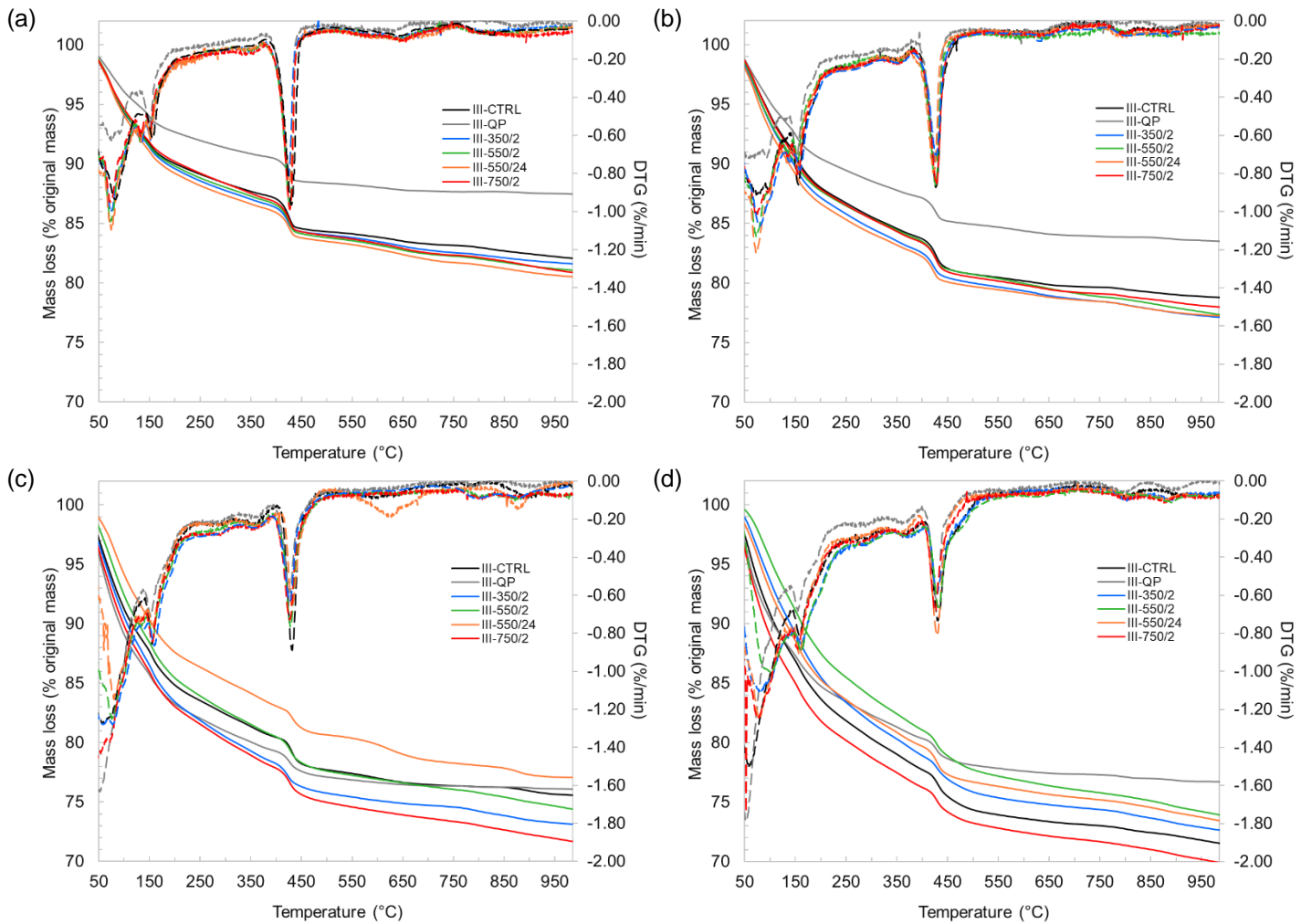


Figure 11. The TGA and DTG curves of the CEMIII pastes. (a) 3 d, (b) 7 d, (c) 28 d, (d) 90 d

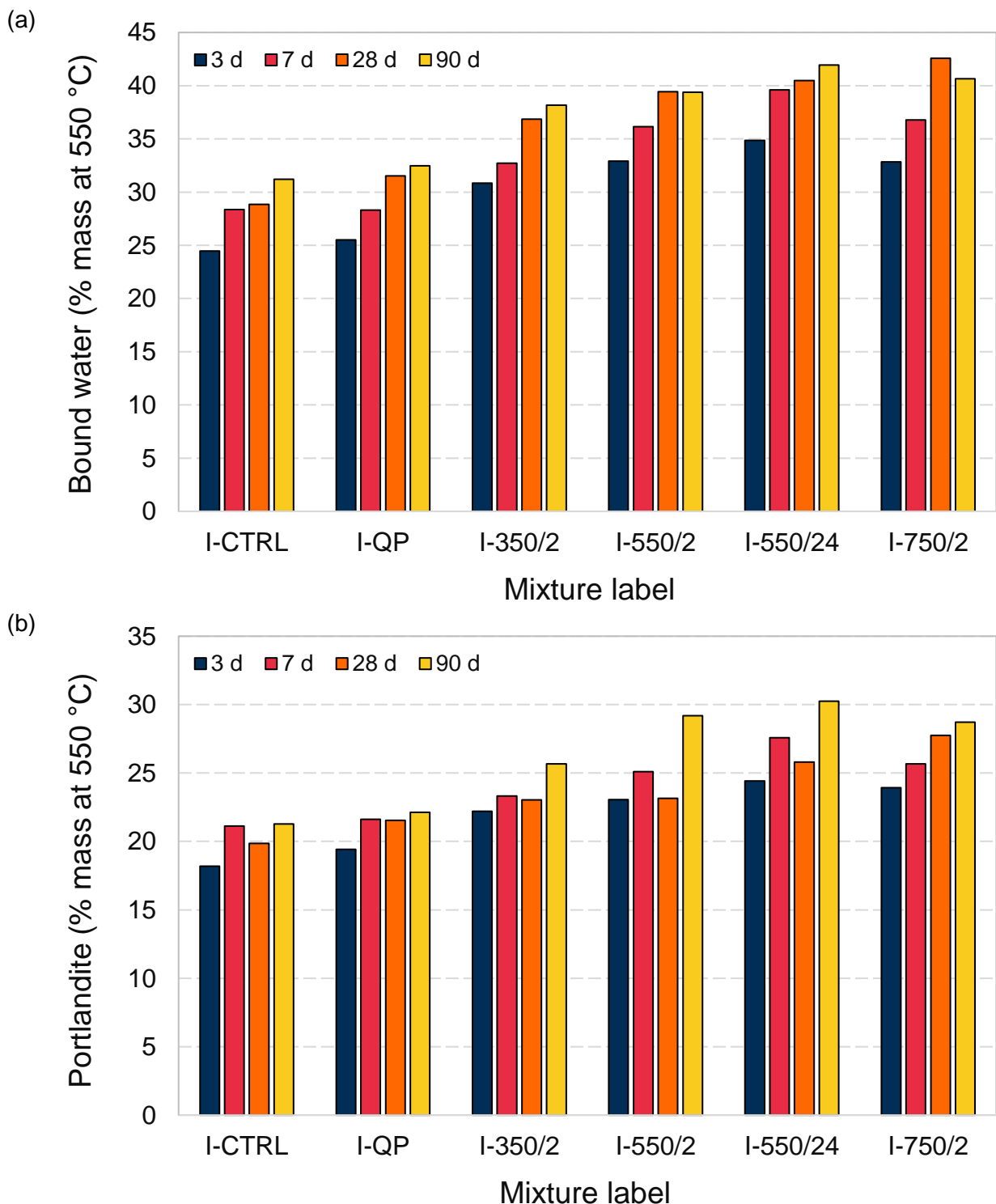


Figure 12. The bound water (a) and portlandite content (b) values of the CEMI pastes (values normalised to the CEMI content in the pastes)

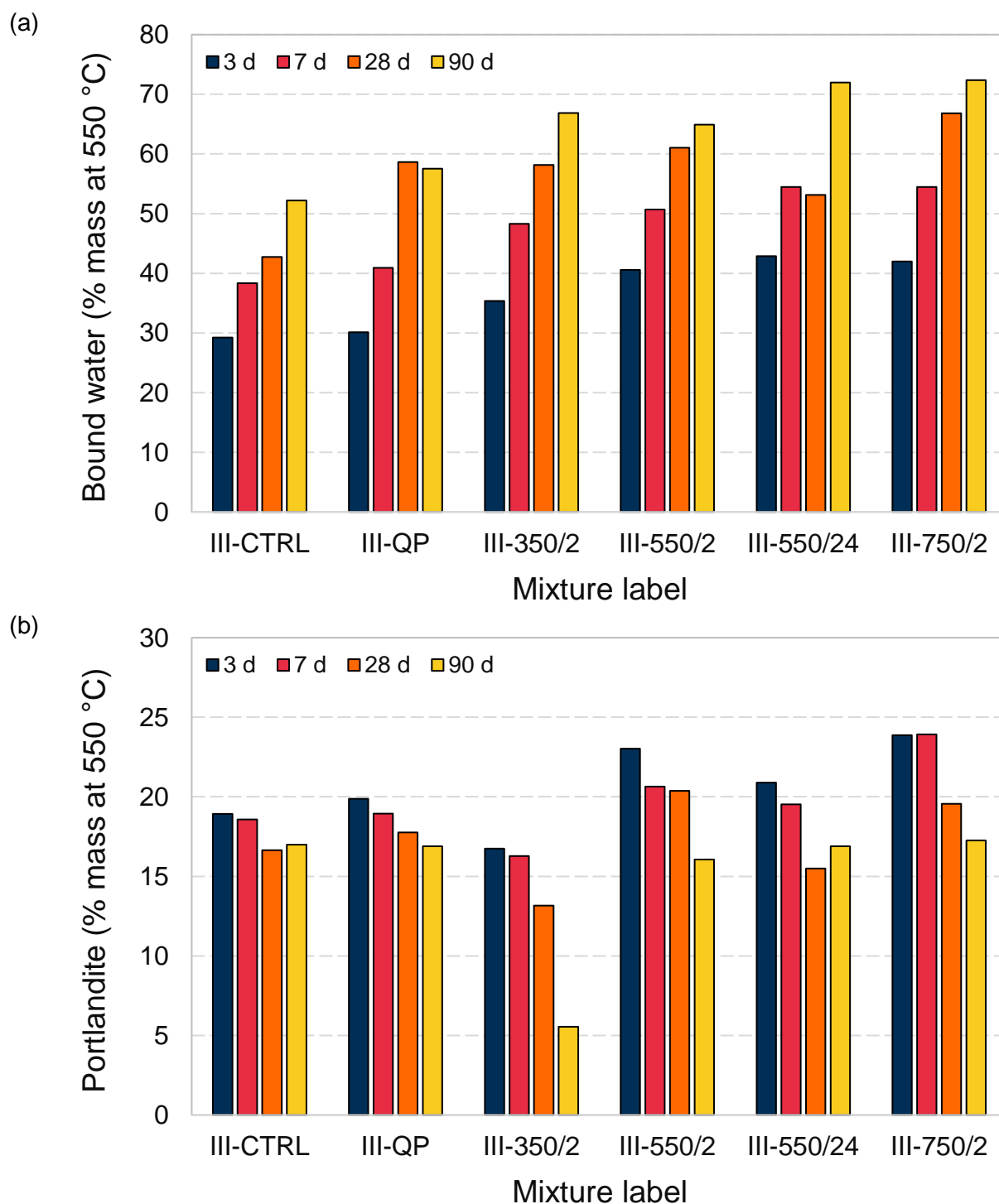


Figure 13. The bound water (a) and portlandite content (b) values of the CEMIII pastes (values normalised to the CEM I content in the pastes)

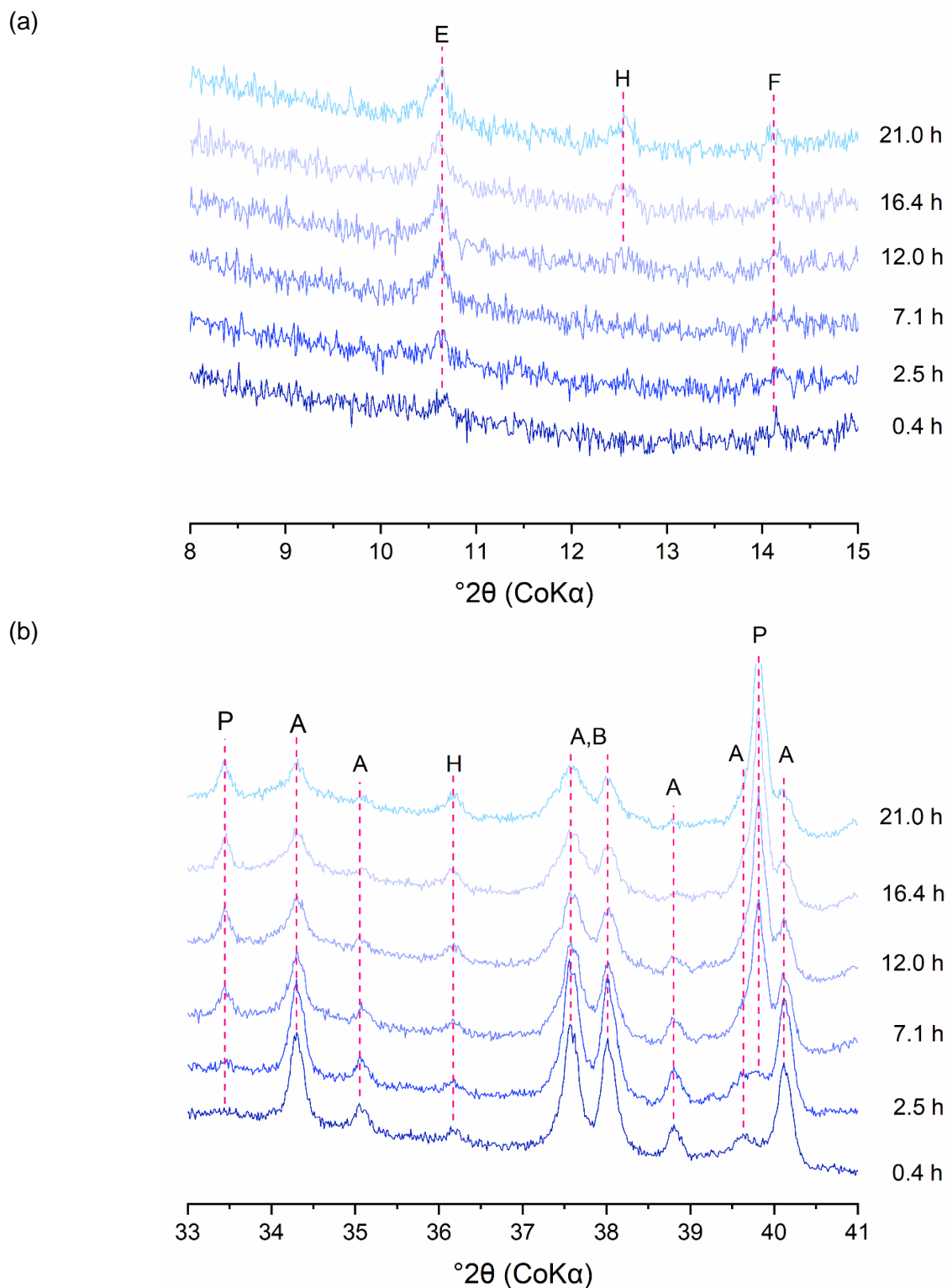
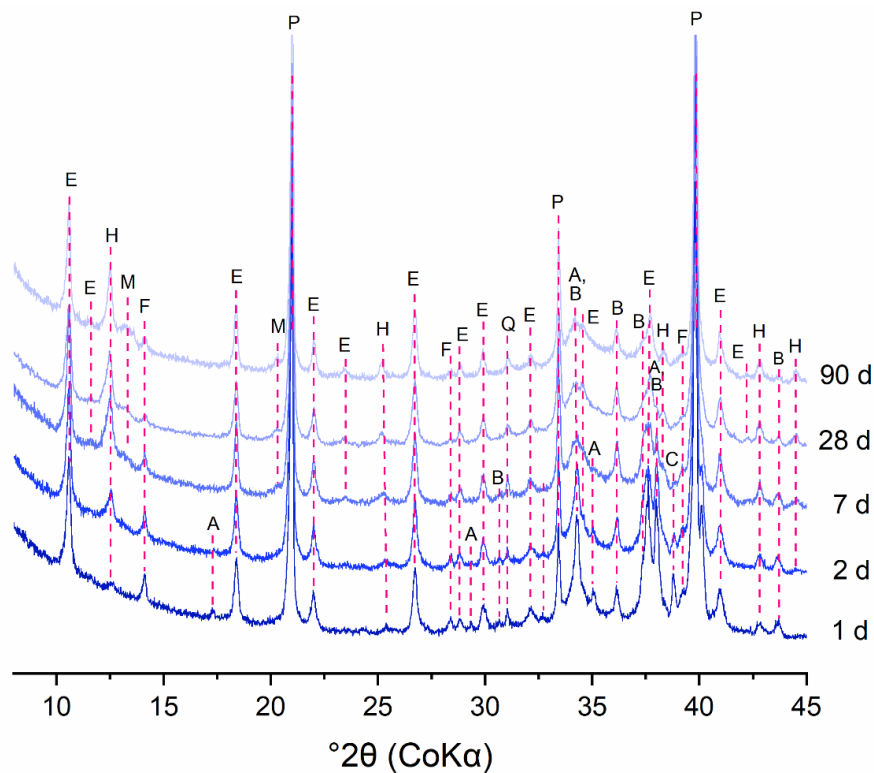


Figure 14. The in-situ XRD pattern of I-350/2 paste over time. (a): 8–15°, (b): 33–41°; A: alite, B: belite, E: ettringite, F: ferrite, H: hemicarboaluminates, P: portlandite

(a)



(b)

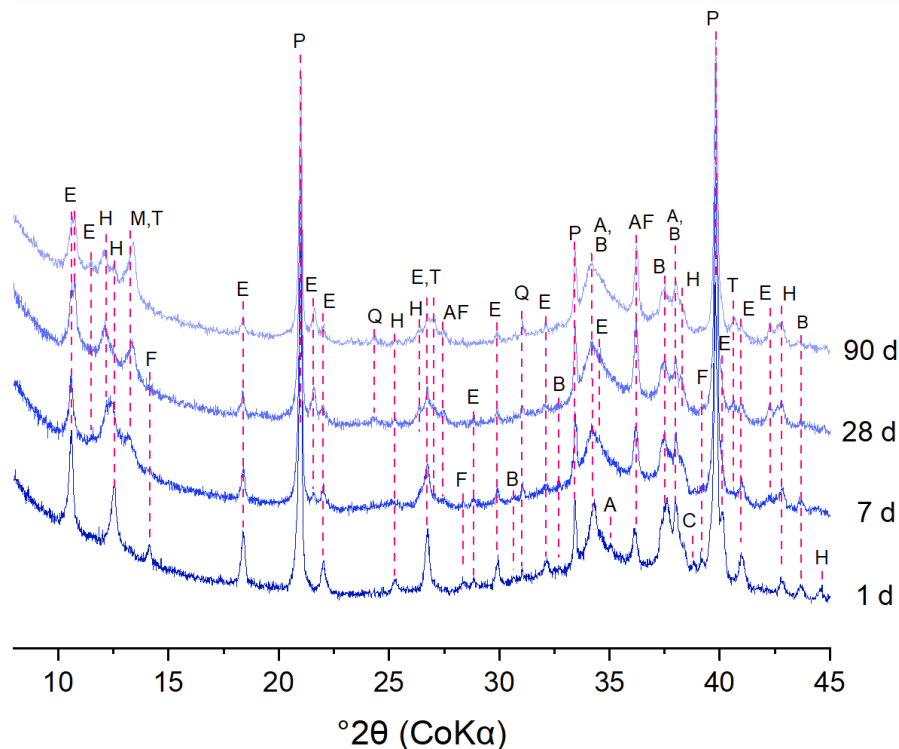
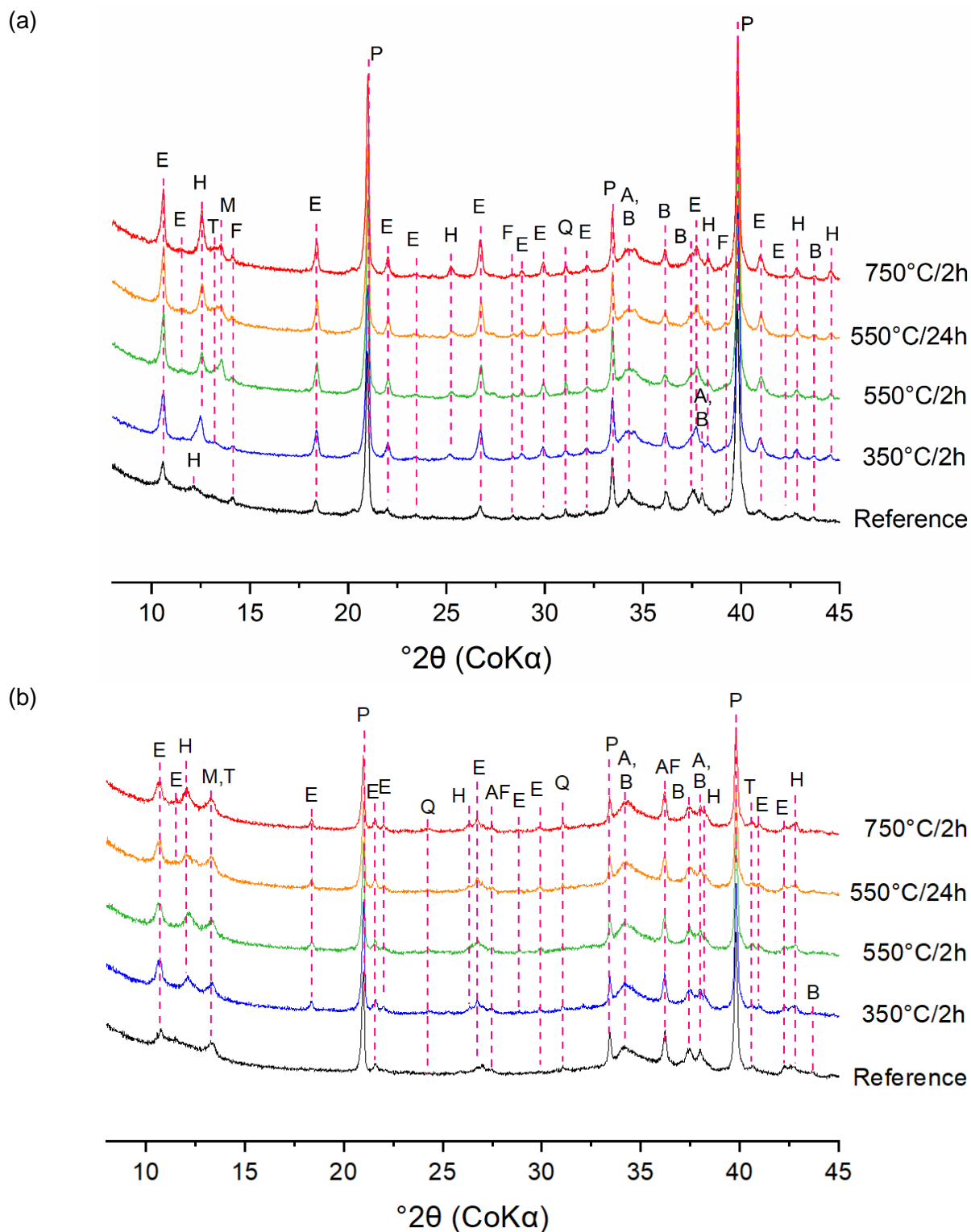
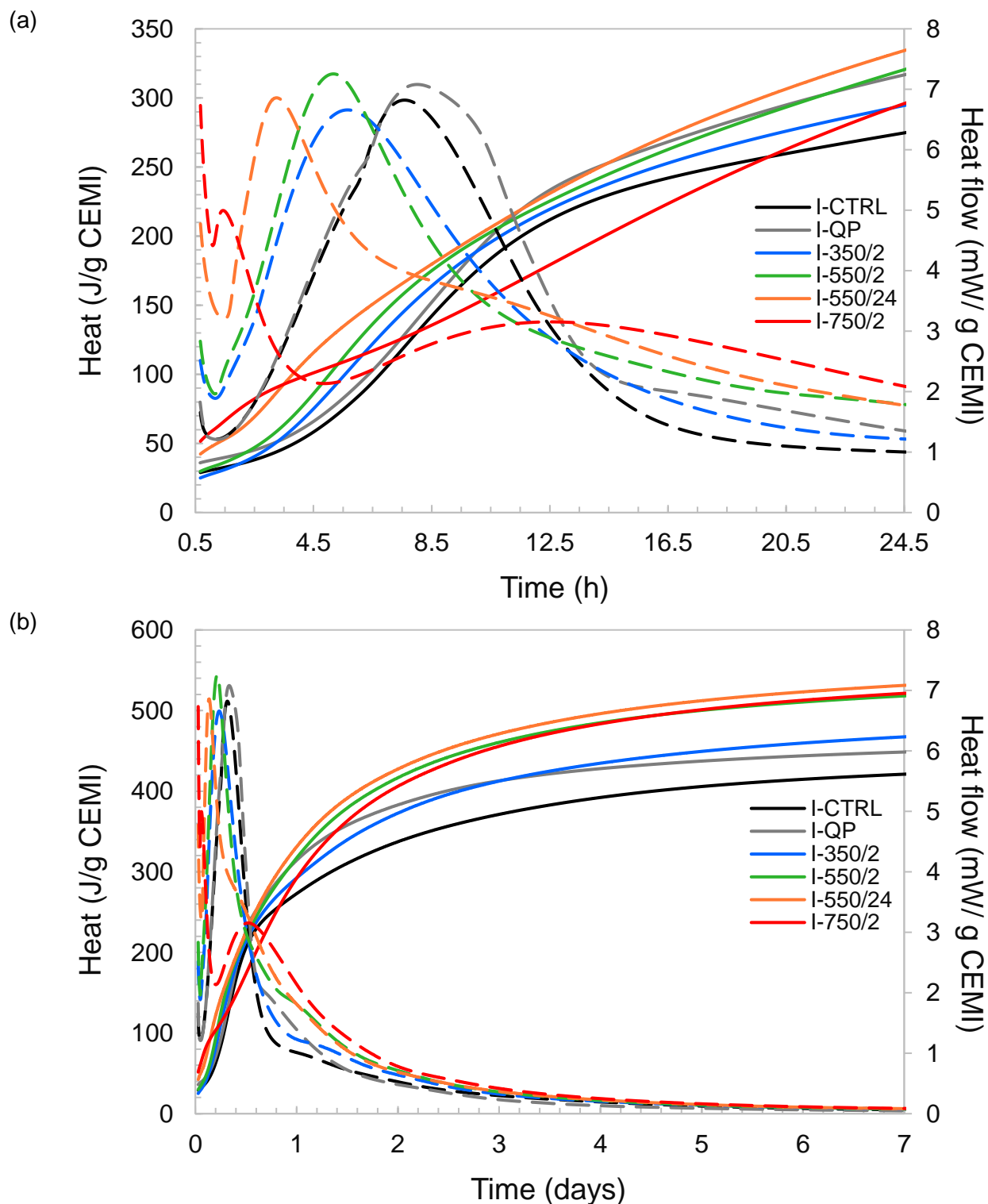
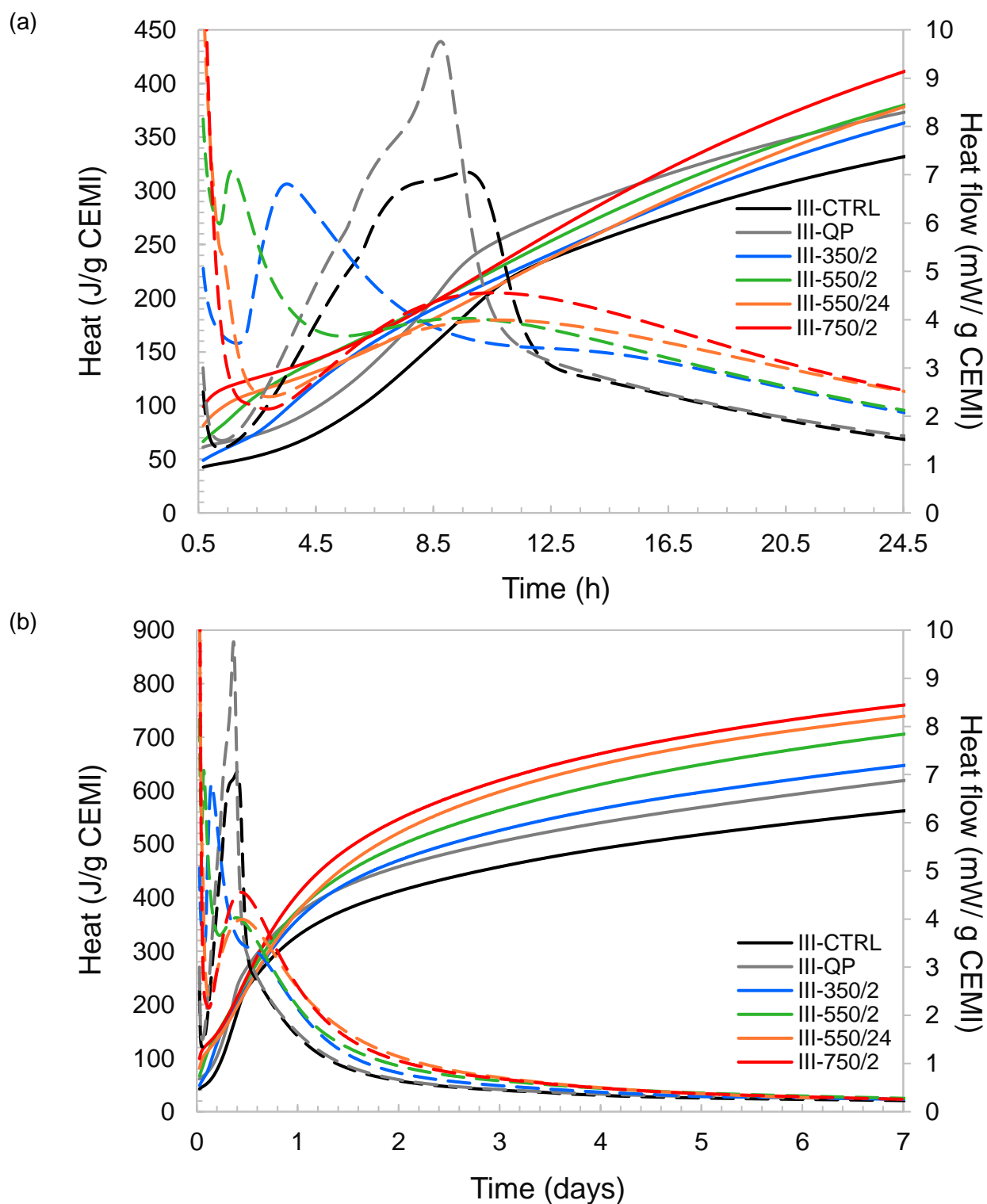


Figure 15. The ex-situ XRD pattern of (a) I-350/2 paste, and (b): III-350/2 pastes over time; A: alite, AF: AFm phases, B: belite, C: C_3A ; E: ettringite, F: ferrite, H: hemicarboaluminates, M: monocarboaluminates; P: portlandite, Q: quartz, T: hydrotalcite







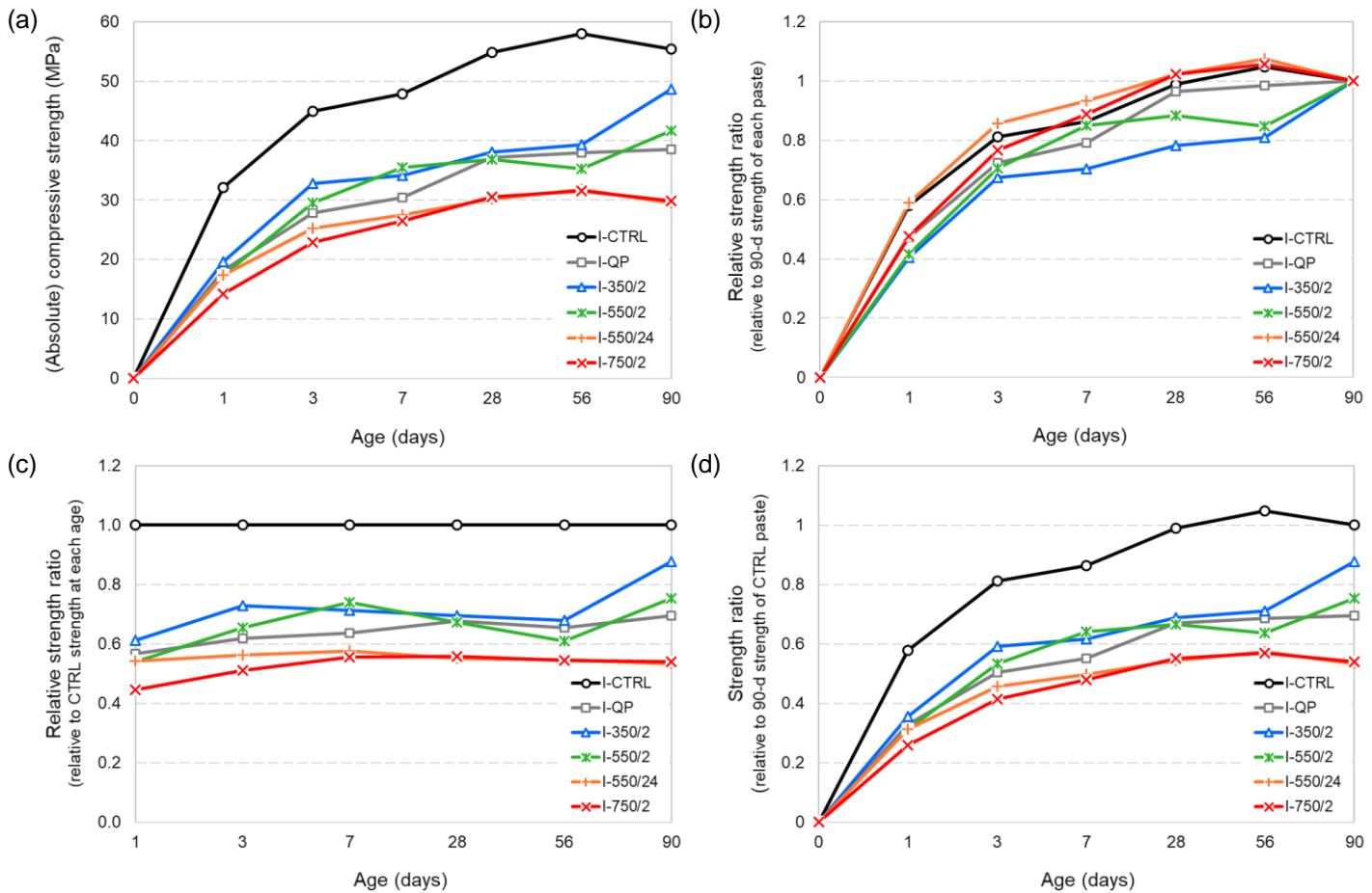


Figure 19. The compressive strength results of the CEMI pastes. (a) absolute compressive strength results with error bars ($=2 \times$ standard deviation), (b) relative strength ratios with respect to the 90-d strength of each respective paste, (c) relative strength ratios with respect to the strength of the control mixtures at the same age, (d) relative strength ratios with respect to the 28-d strength of the control mixture

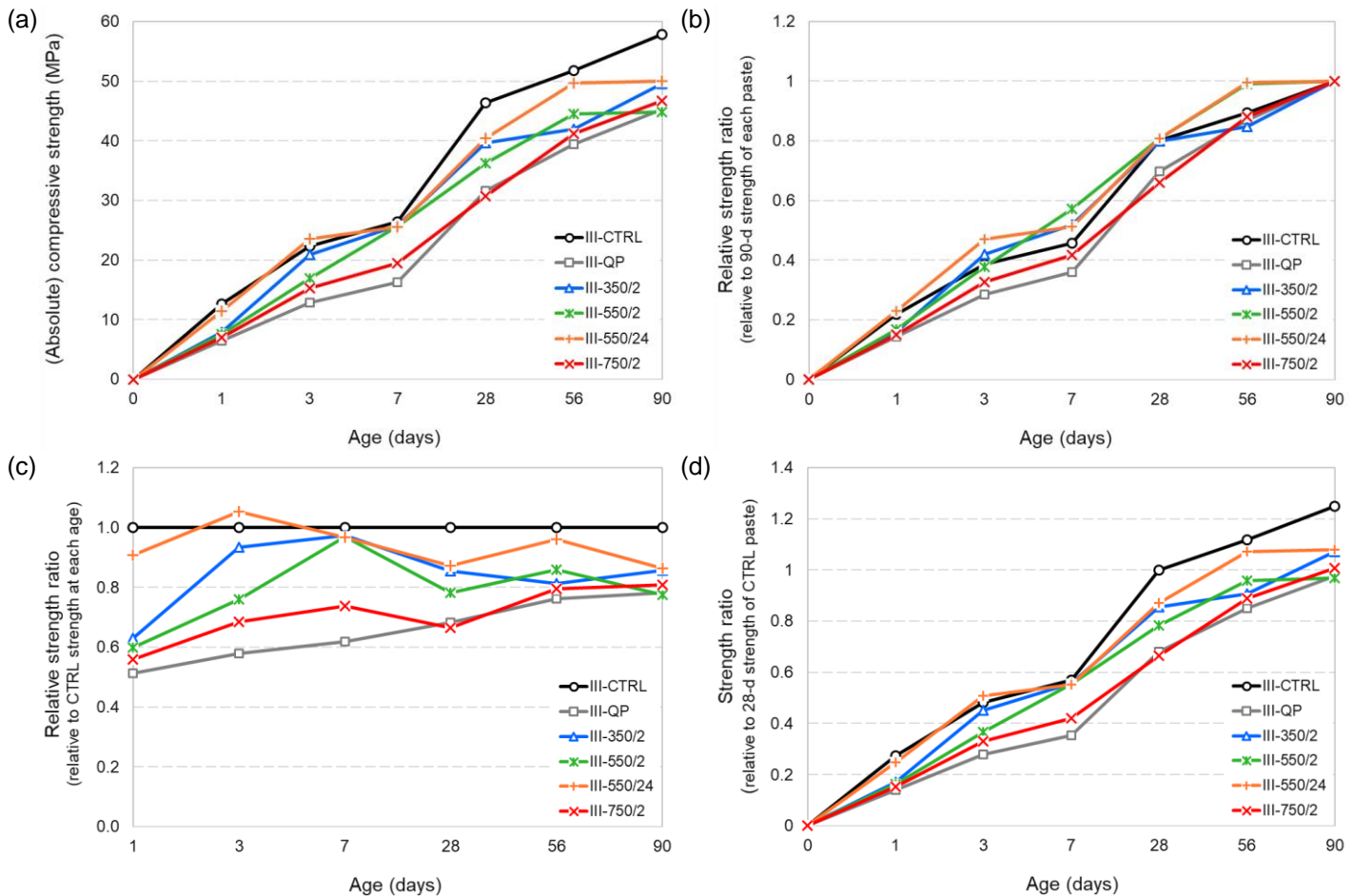


Figure 20. The compressive strength results of the CEMIII pastes. (a) absolute compressive strength results with error bars ($\pm 2 \times$ standard deviation), (b) relative strength ratios with respect to the 90-d strength of each respective paste, (c) relative strength ratios with respect to the strength of the control mixtures at the same age, (d) relative strength ratios with respect to the 28-d strength of the control mixture

References

- [ⁱ] Sanjuán, M. Á., Andrade, C., Mora, P., & Zaragoza, A. (2020). Carbon dioxide uptake by cement-based materials: A Spanish case study. *Applied Sciences*, 10(1), 339.
- [ⁱⁱ] Bribián, I. Z., Capilla, A. V., & Usón, A. A. (2011). Life cycle assessment of building materials: Comparative analysis of energy and environmental impacts and evaluation of the eco-efficiency improvement potential. *Building and environment*, 46(5), 1133-1140.
- [ⁱⁱⁱ] Worrell, E., Price, L., Martin, N., Hendriks, C., & Meida, L. O. (2001). Carbon dioxide emissions from the global cement industry. *Annual review of energy and the environment*, 26(1), 303-329.
- [^{iv}] WBCSD and CSI. *Cement Industry Energy and CO₂ Performance. Getting the Numbers Right* (GNR). 12/30/2016 8/24/2021]; Available from: <https://docs.wbcsd.org/2016/12/GNR.pdf>.
- [^v] Bosoaga, A., Masek, O., & Oakey, J. E. (2009). CO₂ capture technologies for cement industry. *Energy procedia*, 1(1), 133-140.
- [^{vi}] Naqi, A., & Jang, J. G. (2019). Recent progress in green cement technology utilizing low-carbon emission fuels and raw materials: A review. *Sustainability*, 11(2), 537.
- [^{vii}] Recommendation, R. I. L. E. M. (1994). Specifications for concrete with recycled aggregates. *Materials and Structures*, 27(9), 557-559.
- [^{viii}] Gastaldi, D., Canonico, F., Capelli, L., Buzzi, L., Boccaleri, E., & Irico, S. (2015). An investigation on the recycling of hydrated cement from concrete demolition waste. *Cement and Concrete Composites*, 61, 29-35.
- [^{ix}] Schoon, J., & De Buysser, K. (2014). Fines extracted from recycled concrete as alternative raw material for Portland clinker production. In *1st Concrete Innovation Conference (CIC 2014)*.
- [^x] Topič, J., & Prošek, Z. (2017). Properties and microstructure of cement paste including recycled concrete powder. *Acta Polytechnica*, 57(1), 49-57.
- [^{xi}] Oksri-Nelfia, L., Mahieux, P. Y., Amiri, O., Turcry, P., & Lux, J. (2016). Reuse of recycled crushed concrete fines as mineral addition in cementitious materials. *Materials and Structures*, 49(8), 3239-3251.
- [^{xii}] Florea, M. V. A., Ning, Z., & Brouwers, H. J. H. (2014). Activation of liberated concrete fines and their application in mortars. *Construction and Building Materials*, 50, 1-12.
- [^{xiii}] Shui, Z., Xuan, D., Chen, W., Yu, R., & Zhang, R. (2009). Cementitious characteristics of hydrated cement paste subjected to various dehydration temperatures. *Construction and building materials*, 23(1), 531-537.
- [^{xiv}] Wu, H., Xu, J., Yang, D., & Ma, Z. (2021). Utilizing thermal activation treatment to improve the properties of waste cementitious powder and its newmade cementitious materials. *Journal of Cleaner Production*, 129074.
- [^{xv}] Snellings, R., & Scrivener, K. L. (2016). Rapid screening tests for supplementary cementitious materials: past and future. *Materials and Structures*, 49(8), 3265-3279.